Journal of Alloys and Compounds 876 (2021) 159939

Contents lists available at ScienceDirect

Journal of Alloys and Compounds

journal homepage: www.elsevier.com/locate/jalcom

Review

Thin film metallic glasses for bioimplants and surgical tools: A review

S. Thanka Rajan*, A. Arockiarajan*

Department of Applied Mechanics, Indian Institute of Technology Madras, Chennai 600036, India

ARTICLE INFO

Article history:
Received 15 March 2021
Received in revised form 7 April 2021
Accepted 9 April 2021
Available online 18 April 2021

Keywords:
Metallic glass
Thermal stability
Mechanical property
Biocompatibility
Hemocompatibility
Corrosion
Mineralization

ABSTRACT

Amorphous thin film metallic glasses (TFMGs) have given rise to a widespread research interest due to their technological promise for practical applications and scientific importance in the biomedical field. As a result of their disordered atomic structure (leading to amorphicity), these TFMGs symbolize a new class of structural and functional materials with extraordinary properties, including exciting strength along with superior mechanical properties and biological properties. TFMG top-coats have the potential to improve the strength, corrosion resistance, biocompatibility, and life span of potential biomaterials (metallic, ceramics, or polymers). This article reviews the mechanical properties and biological behavior of TFMGs as well as the current progress in Zr-based, Ti-based, Fe-based, and Mg-based TFMGs for biomedical applications.

Contents

* Corresponding authors.
E-mail addresses: strajan984@gmail.com (S.T. Rajan), aarajan@iitm.ac.in (A. Arockiarajan).

https://doi.org/10.1016/j.jallcom.2021.159939
0925-8388/

1. Introduction

Bioimplants are devices fabricated as support to injured biological structures or a substitute for a missed biological part. The material may be a combination of natural or inorganic, or organic elements that are biocompatible and help humans throughout the healing duration [1]. The biomaterials are used in restoration function and enhance the field of medicine and dentistry. The utmost established and trusted materials that are accepted to be used as biomaterials are metals and metal alloys, polymers, and ceramics. All the materials have their own unique properties along with pitfalls in their respective field of application.

The minimum requirement for a successful implant is to avoid adverse tissue reaction, strength, resistance to degradation, and wear and modulus closer to bone [2]. Metals and metal alloys are the appropriate materials for bearing loads due to their strength and wear resistance, which is mostly used as a substitute or fixe bone implants. Stainless steel (SS 316L), Ti and its alloys, and Cobalt-chrome (CoCr) alloys are the metallic components used as bioimplants and for biomedical application [3,4]. The low carbon SS (316L) is a biocompatible material due to the formation of a passive layer of chromium oxide and highly resistant to corrosion, and has good strength. When compared to SS, CoCr alloys have a longer implant duration time and are more averse to encounter fatigue fracture [3]. Ti and alloys are extensively used in the biomedical field due to their lightweight, strength, and resistance to corrosion [5]. Osseointegration is a unique property of Ti and its alloys which is the direct interface between an implant and bone without any ligament fibers or cartilage and scar tissues existing between the implant and bone [6]. The tissue compatibility of Ti was verified by calcium phosphate formation ability in simulated body fluids [7]. Adhesion and proliferation of osteogenic cells are due to the wettability, surface morphology (roughness), etc., which are important factors prevailing hard-tissue compatibility. The bone formation takes place via three stages the initial one is the inflammatory response period, and the next is the induction period, and finally, bone formation [8]. The composition and chemical state of the surface oxide film of the implant varies according to the surrounding environment, while the film is macroscopically stable. A passive film maintains a continuous process of partial dissolution and re-precipitation in the electrolyte so, the surface composition is always changing according to the environment [9].

When a material is placed in biological environs, it should exist without any contrary effect, which is the essential requirement of a biomaterial. The biomaterial's surface is the interface that interacts with the physiological surroundings (blood, bone, and tissue), which is the ultimate factor for refusal or acceptance of a material in the human. The material implanted in the human tries to isolate it by wrapping it in fibrous tissues (fibrous layer formation), weakening the bond formation between the implant and the tissues close to it and leading to implant failure [10]. The additional problem in implants is their corrosion property, leading to metal ions' release, causing inflammation [11]. Biocompatibility and bioactivity depend on the surface properties of the biomaterial. To make the implant surfaces more bioactive, compatible, and enhance their properties, surface modification is an effective method to protect them in body environs. Surface modification is an important and efficient way to overcome wear and degradation properties in the biomedical field. Thin film fabrication techniques will be employed to coat various efficient coatings on the implant surfaces that can significantly change their morphology, composition, and structure. Multiple kinds of thin film coating techniques comprise wet chemical coating methods like sol-gel, dip coating, CVD (chemical vapour deposition), etc. and PVD (physical vapour deposition) like sputtering, evaporation, PLD (Pulsed laser deposition) etc. [12]. Metallic glasses (MGs) are potential candidates for biomedical applications since they are amorphous in nature, have improved wear and corrosion resistance, and avoids stress shielding.

2. Bulk metallic glasses (BMGs)

Decades before researchers found interest in MGs for medical application, these were used in widespread areas like jewellery and sports equipment etc. MGs are the fast cooled molten alloy that suppresses the crystalline nucleation phases and forms glassy alloys. The glassy alloys are unusual metallic materials that are amorphous and exhibit discrete atomic order arrangement compared to crystalline materials [13]. The amorphous MGs possess worthy features like greater strength and resistance to degradation or corrosion [14]. After the glass transition temperature (T_g) and before the crystallization temperature (T_x) and crystallization event, MGs are softer and more formable but amorphous. The region between T_g and T_x is the supercooled liquid region (SCLR). In this region, the MGs can be shaped by applying a small force using processing techniques like forming, extrusion, injection blow moulding before cooling to solid MG [15]. The fast cooled alloy system frameworks offer improved mechanical and anti-corrosion properties. The alloy composition can be prepared with nontoxic elements to make them more biocompatible and bioactive [16]. The MGs have better properties than existing biomaterials in surgical instruments and implants used in the load-bearing application. MGs have a high elastic strain limit of 2% compared to the bone of 1% [17]. Their modulus of elasticity is

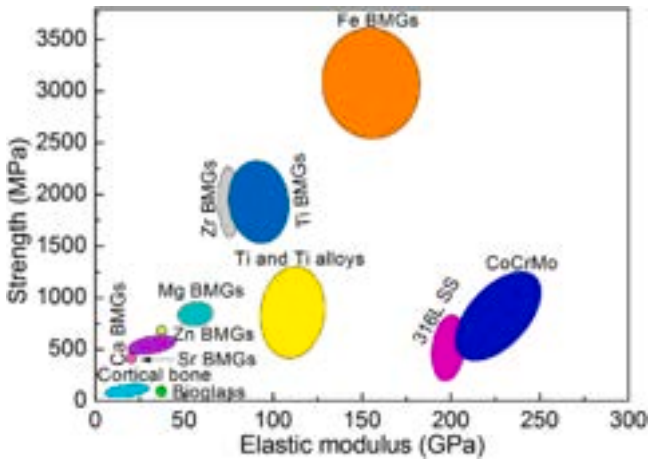

Fig. 1. The comparison of the mechanical properties of crystalline metals alloys and BMGs with the human bone [19].

nearer to the bone and avoids the stress shielding which favours hard-tissue prostheses [18]. The MGs exhibit an extraordinary elastic limit of ~2% compared to bone (~1%) [17]. It proposes that MGs are more flexible with the usual twisting and bending of the bones and subsequently transfer stress more uniformly than metallic biomaterials and reduces stress and stress shielding effects, and heals faster [19].

Fig. 1 elucidates the comparison of elastic modulus and strength of the conventional crystalline alloys, metals and BMGs with human bone. Fig. 1 displays that the BMGs have high strength and low elastic modulus compared to traditional crystalline materials, which makes them highly appropriate for bioimplants application [19]. The first metallic glass of $Au_{75}Si_{25}$ was fabricated by Klement et al. by fast quenching of metal alloy molten liquid with a cooling rate of 106 K/s in 1960 [20]. The initially stated BMG was fabricated by Chen et al. They prepared Pd–Cu–Si BMG of the diameter 1–2 mm specimens with glassy nature and stability against crystallization reflected with greater reduced glass temperature (T_{rg}) [$T_{rg} = (T_g/T_l)$] [21]. Later extensive research was performed in investigating MGs with higher glass forming ability (GFA) and good mechanical property.

A couple of decades after, a wide range of different alloy compositions were formed as glassy metals, like Pd, Zr, Cu, Fe, Ni, Ti, Co, Au and Mg-based glassy alloys by different solidification approaches [15,22]. MGs which can be used for biomedical application should be nontoxic or free of harmful materials like Be, Ni, Cu, and Al and mostly Ti, Zr, Fe- based BMGs are used as non-degradable biomedical materials [23]. The controlled degradation and nontoxic nature, along with biocompatibility and bioresorbable interaction with hosts, make Mg-based BMGs an appropriate biodegradable biomaterial [24,25].

3. Thin film metallic glasses (TFMGs)

The finding of MGs has inspired unavoidable extensive research due to their scientific and technological significance in understanding the knowledge of glass metals development. Since BMGs are tough to fabricate as a sheet thicker than 10 mm or bigger, or difficulty in moulding into complicated sizes impedes its real-time applications and commercialization. The cooling speed (critical cooling rate) required to solidify molten liquid melt without inducing crystallization is inverse to the square of the thickness $(1/t^2)$ and proportional to thermal diffusivity (κ) of the sample (κ): $\dot{T}_{cr} \propto \kappa/t^2$ [26]. The critical cooling rate ranges from 150 K/s to 1 K/s or lower; for nominal values of thermal diffusivity (κ) [27]. So, to get homogenous MGs κ and thickness of the material are the crucial factors.

Condensing vapour atoms can prepare thin films of the MGs to solid thin films of amorphous layers on different substrates. The thin film deposition process is in more equilibrium compared to the molten liquid quenching or casting process. The vapour to solid condensation route favours MG alloys' formation with supersaturated immiscible elements without any problem. These systems are different from the constant or rapid cooling of molten melt and constrained into a sudden energy gradient by a change in phase directly from vapour to solid by avoiding the intermediate formation of a liquid phase. The phase formed is amorphous in nature, and their compositions are near similar to the BMG components, and they are called thin film metallic glasses (TFMGs) [26]. Often, they fill the need of BMGs yet with the help of the underlying substrate. Surface modification of the crystalline biomaterials with TFMGs gives a simple way to avoid the fabricating obstacles related to BMGs, but achieve the ultimate properties of metallic glasses. In the biomedical field, the most essential is the surface properties such as corrosion resistance which coatings of TFMGs can very much improve on to mechanically compliant materials [28]. When the MGs are fabricated as thin film, they have improved GFA and offer a range of composition for amorphous films. Their favourable fabrication techniques include physical vapour deposition methods like sputtering, PLD, etc. [29,30].

Vacuum coating methods like sputtering involve the target materials' atoms being transmitted to the substrates through ion bombardment and the atoms layers are condensed as a thin film. The atomic transformation in the sputtering process has a greater cooling rate than regular cooling of the liquid molten material to a solid process which is a possible approach for TFMG [31]. The sputtering technique avoids microsegregation and nanocrystallization. This process offers dense coatings and films with a good bond to substrates, and TFMGs fabricated are uniform with control over their elemental compositions; the mixing the elemental atoms in the thin film [32]. The combinatorial sputtering process can tune a large number of compositions and variations in microstructure, and it is a favourable way for the formation of TFMG systems [33].

PLD (pulsed laser deposition) method with a laser at high vacuum is a scalable and reliable technique for fabricating thin films. PLD is a flexible process as several types of materials can be deposited, and any material can be used as a substrate. Also, it enables microstructure ranging from crystalline to entirely amorphous [34]. Furthermore, PLD can be employed to grow complex compositions by congruent vaporisation, ensuring that the film grown replicates the same composition as that of the target. This process is predominantly appropriate for noble metal-based amorphous coatings comprising metalloids like boron, which are challenging to coat by other thin film coating or deposition processes [34,35].

Developing of TFMGs has gained attention in making it and overcoming the hurdles of the BMG, such as fabrication of bigger or complicated size. TFMGs with good corrosion resistance, GFA and improved stability in tissues integrate with different living tissue (biocompatibility), which are potentially suitable for biomedical applications. Fig. 2 shows the aim of enhancing biomaterial performance by TFMG and displays their types. TFMGs properties and biocompatibility have been investigated by researchers

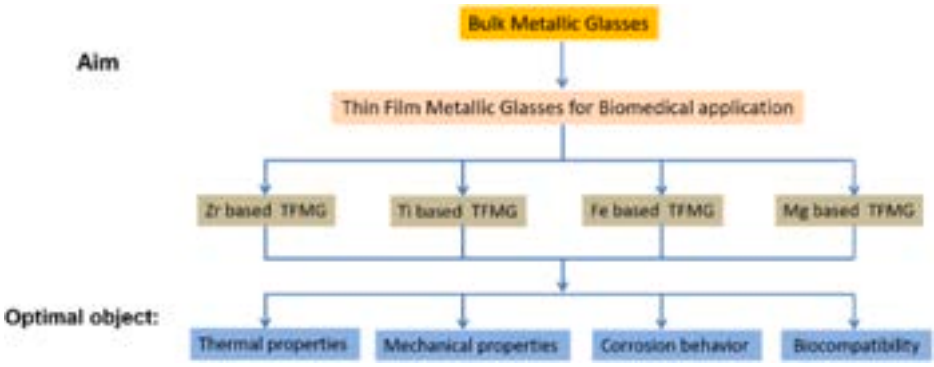

Fig. 2. Directions of improvements on biomaterials by TFMGs and their studies done.

Table 1
Description of the focus points of some review articles published since year 2005 on TFMGs.

Year	Name of the authors	Focus points legends: (●-Present, ×-absent)	Discussion of thermal property	Discussion of mechanical property	Discussion of corrosion property	Discussion of biological studies	Reference
2010	Chu et al.	➢ TFMGs fabrication and properties ➢ TFMG explored for MEMS applications ➢ Interatomic potentials are derived by simulations	×	●	●	×	[36]
2012	Chu et al.	➢ TFMGs are of high strength, large plasticity within ΔT, and excellent wear resistance ➢ TFMGs includes solid-state amorphization upon annealing ➢ Potential applications in microelectronics and optoelectronics.	●	●	×	●	[33]
2020	Yiu et al.	➢ Tunable composition and related property enhancements ➢ Tribological and surface properties of the TFMG ➢ Superior plasticity and ductility ➢ Enhancing the fatigue life of engineering alloys ➢ Medical needles and guidewires	×	●	●	●	[37]
2020	Korkmaz et al.	➢ Production and structure of Zr based thin film metallic glasses ➢ Thermal properties of Zr-based thin film metallic glasses ➢ Examination of the mechanical properties Zr TFMG	●	●	×	×	[38]
2021	Rajan et al. (This article)	➢ Thermal properties of MGs are more significance due to its role for the thermal stability and glassy nature. ➢ The mechanical properties of TFMG attain excessive prominence. ➢ The chemical stability of the TFMG was assessed by the corrosion studies ➢ TFMGS properties and biocompatibility have been investigated ➢ Biodegradable metallic glasses	●	●	●	●	[Present article]

systematically and reported. Table 1 presents a comprehensive discussion about the TFMGs and the focus points of the studies. The current review sums up and discusses the development made in the region of different types of TFMGs as biomaterials in the previous years.

4. Zr-based TFMGs for bioimplants and devices

4.1. Thermal properties of Zr-based TFMGs

Among different types of ternary and quaternary MGs, Zr-based MGs have extraordinary GFA with a large SCLR. The binary MGs of Zr based systems like Zr-Cu have greater GFA, which leads to an extensive glass-forming range [39]. The GFA was also influenced by APD (atomic packing density), in which the MGs structural stability is associated with its native arrangement of atoms. This outcome of APD correlated to Cu-Zr MG properties is reported by Park et al. [40]. Rauf et al. proposed the reason for improved thermal stability of the Cu-Zr MGs against crystallization. The difference in the atomic size of atoms of Zr and Cu (0.155 nm and 0.135 nm) is densely packed. It leads to a local atmosphere around Cu and Zr molecules away from the contending structure crystalline phase, [41] thereby avoiding crystallinity. Zr–Ni–Al-Si TFMGs were fabricated by C.-Y. Chuang et al., who elucidated the XRD and DSC outcomes of the coatings with different nitrogen flow rate or percentage of target poisoning. Fig. 3a. showed the amorphous nature of ZN-0 and ZN-1, and the other specimens are crystalline. The DSC curves displayed (Fig. 3b.) T_g and T_x when they are amorphous, and the crystalline specimens do not display T_g and T_x representing the absence of a glassy amorphous state [42]. Only the amorphous glassy films show the glass transition in the thermogram. Rajan et al. stated a T_{rg} (reduced glass transition temperature) of 0.3473 for Zr-Cu-Ag-Al TFMGs. They suggested not only T_g and T_x values; T_{rg} is also a pointer of the alloy to form MG. Typically the thumb rule for predicting GFA of MGs is $T_{rg} > 2/3$ [26]. This criterion is relaxed for TFMGs due to vapour phase condensation, deviation in composition and adatom probability on the substrate's surface [26].

4.2. Mechanical properties of Zr-based TFMGs

The orthopaedic biomaterials are used in various biological conditions like loadings and wear from the biological environment. The hardness of different BMGs and corresponding Youngs modulus is displayed in Fig. 4. The hardness and modulus of the BMGs are nearly equal to the crystalline titanium, and Zr based TFMGs also show the same hardness (3–6 GPa) and Youngs modulus of (80–130 GPa) [43]. The summary of the mechanical properties of Zr based TFMGs and BMGs are displayed in Table 2. Chen et al. studied the nitrogen incorporated Zr-Cu-Al-Ag-Ta TFMGs where the nitrogen atoms centred short-range order (SRO) arrangements of atoms leading to a rapid rise in hardness. The nitrogen atoms centred structures showed greater elastic modulus due to the reach of lower configuration potential energy [44]. Similarly, Chuang et al. also found the hardness and modulus increases with an increase in nitrogen for Zr–Ni–Al-Si TFMGs (Fig. 5) due to the formation of nanograins of crystalline ZrN [42].

The scratch test tests the adhesion of the TFMGs to the substrates. Liu et al. coated ZrCuAlNi TFMG on SS and measured the scratch resistance of TFMG, and reported that the shear bands nucleation, formation and propagation are responsible for the ploughing and wear deformation behaviour [58]. The scratch resistance of Zu-Cu-Ag-Al TFMGs is verified by critical loads (Lc), acoustic emission and the depth of penetration of the coatings [26,31]. The tribological characteristic of ZrCuFeAlAg TFMG was studied by Cai et al. in dry and artificial saliva conditions using a ball on plate technique. The fretting wear rate of the TFMG was 2.8 times

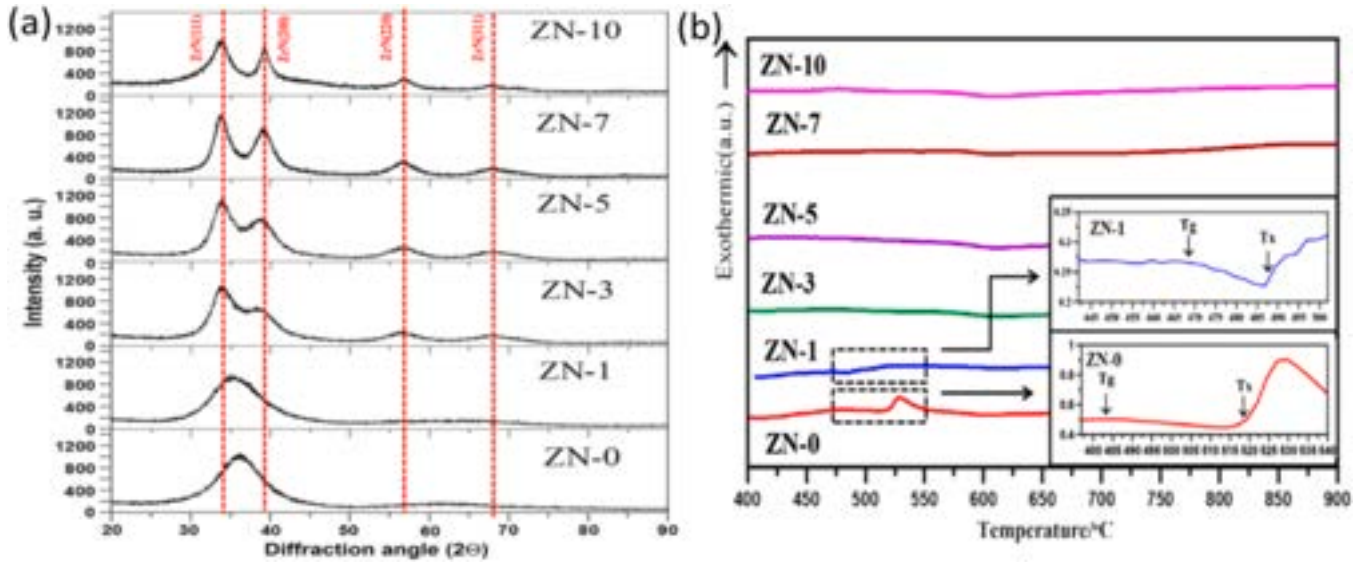

Fig. 3. (a) The XRD patterns and (b) The DSC thermogram for the Zr-based TFMGs [42].

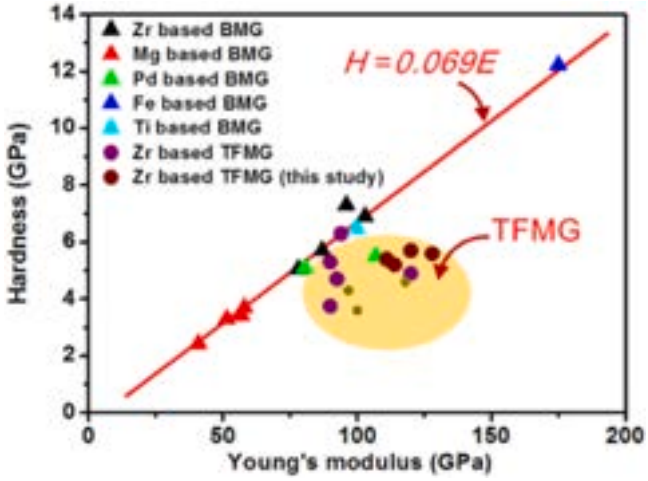

Fig. 4. The hardness and Youngs modulus of different BMGs and Zr based TFMGs [43]. Reproduced from [J.C. Ye, et al., J. Appl. Phys. 112 (2012) 053516], with the permission of AIP Publishing.

inferior in the air or dry condition, and in artificial saliva (wet condition) wear rate is lower as 1.8 times even at the higher coefficient of friction which displays improved fretting wear resistance [47].

TFMG coated surgical blades' sharpness can be assessed by the blade sharpness index (BSI). BSI is the ratio of external load applied to work done to the necessary energy needed to propagate a cut in the material. Tsai et al. evaluated the sharpness of blade made of BMG and TFMG coated SS blade and revealed that both BMG blade and TFMG coated blade showed lower BSI (0.25 and 0.23) when compared to the uncoated SS blade (0.34), which corresponds to 26.5% improvement on blades' sharpness [59]. Later he coated two types of Zr based TFMGs of different thickness and found the coated blades are durable after 20 cm cut, and the BSI was less than 0.45, which suggests the coatings increase the sharpness and durability [60]. Chu et al. reported $Zr_{53}Cu_{33}Al_9Ta_5$ TFMG coated needles of the syringe and compared them to coatings of titanium nitride and titanium. TFMG coatings revealed the insertion force was reduced to ~66% and ~72% for retraction force with lower COF (coefficient of friction) as displayed in Table 3, and the non-sticky nature of the TFMG coated needles with very low friction was referred in Fig. 6 [61].

The non-stick nature of the TFMG coated needles was studied in vitro by a mouse model whose skin is similar to human skin. The images (Fig. 7A-D) represent the puncturing of mouse dorsal skin by uncoated needle and TFMG-coated needle. The tissues clearly stuck to the uncoated needles (Fig. 6a, b); elevated tissue area referred to as a hump during retraction. The TFMG coated needles displayed (Fig. 7C, D) no observable hump clearly illustrating the non-sticky nature. The cells' adhesion to the TFMG coated needle was 79.6% lower than that in the bare needle, which was attributed to the non-stick behaviour. The anti-adhesion performance of the TFMG is originated from the smooth and grain boundary-free surface, as well as the low surface energy [62].

4.3. Corrosion studies of Zr-based TFMGs

The corrosion property of Zr based TFMGs were studied in different physiological environments such as SBF [31,63,64], 5.0 wt% aqueous NaCl solution [65], artificial saliva [47], phosphate-buffered saline (PBS) [66], 1M HCl [67] and Hanks solution [28,64]. It was witnessed that the TFMG coated specimens showed low corrosion current density (I_{corr}) and higher corrosion potential (E_{corr}) when compared to the crystalline materials like stainless steel, Ti and Ti alloys. This suggests that the Zr based TFMGs are more corrosion resistant in different physiological solutions and indicates they are more protective when coated on to crystalline substrates[31,52,63]. When the Zr TFMG is immersed in an electrolyte, a passive layer is formed on the TFMG surface, which is mainly a stable layer composed of ZrO2. A minimum amount of addition of Ag [68] and /or Nb [69] stabilizes and resists the dissolution of ions and improves the resistance to corrosion in different solutions. Rajan et al. studied the corrosion resistant property of $Zr_{48}Cu_{36}Al_8Ag_8$ (at%) TFMG by immersing it in to SBF for 21 days and noticed that the potential rises more nobler for the coatings and the coatings immersed in SBF[52]. Two types of ternary TFMGs corrosion property was studied by Jabed et al. in PBS and sodium sulfate solutions which demonstrated an inferior passive current density and corrosion [46]. The corrosion or degradation of the material was mostly affected by the amorphous nature and formation of oxides of Zr, Ti, Al and Ag on the surfaces. The corrosion mechanisms of the Zr-based TFMG were discussed by Chuang et al. The surface morphology of the coatings after the corrosion test showed river-flow shapes and cracks tending to pitting and crevice corrosion with filiform reaction(Fig. 8) [67].

Table 2
Summary of mechanical properties of Zr-based TFMG and BMG systems.

Chemical composition (at%)	Elastic modulus GPa	Hardness GPa	Vickers hardness (Hv) (kg mm^2)	Yield strength (GPa)	Reference
TFMGs					
$Zr_{53}Cu_{29}Al_{12}Ni_6$	117	5.5	–	2.6	[43]
$Zr_{52}Cu_{48}$	97	5.4	–	–	[45]
$Zr_{86}Cu_8Ag_6$	78	4.2	–	–	[45]
$Zr_{73}Cu_{16}Ag_{11}$	80	4.3	–	–	[45]
$Zr_{47}Cu_{28}Ag_{25}$	110	5.9	–	–	[45]
$Zr_{46}Ti_{40}Ag_{14}$	109.15	6.12	–	–	[46]
$Zr_{46}Ti_{43}Al_{11}$	126.5	5.61	–	–	[46]
$Zr_{60.14}Cu_{22.31}Fe_{4.85}Al_{9.7}Ag_3$	116.1	7.0	–	–	[47]
$Zr_{41.1}Ni_{30.3}Al_{1.3}$ $Si_{5.2}$ $N_{17.7}$	223	14.7	–	–	[42]
$Zr_{48}Cu_{52}$	123	5.2	–	–	[48]
$Zr_6Cu_7Ni_{43}Al_{44}$	159	8.2	–	–	[48]
$Zr_{50}Cu_{50}$	98	6.2	–	–	[49]
$Zr_{52.2}Cu_{30.4}Ni_{8.6}Al_{8.8}$	112	4.7	–	–	[50]
$Zr_{32}Cu_{20}Al_8Ni_5N_{35}$	190	9.5	–	–	[51]
$Zr_{33.4}Cu_{17.6}Al_{5.4}Ni_{4.1}B_{12.3}N_{26.8}$	219	15.1	–	–	[51]
$Zr_{48}Cu_{36}Ag_8A1_8$	112.6	8.92	–	–	[52]
BMGs					
$Zr_{64}Cu_{16}Ni_{10}Al_{10}$	113 GPa	–	–	–	[53]
$Zr_{61}Cu_{17.5}Ni_{10}Al_{7.5}Si_4$	–	–	510	–	[54]
$Zr_{60+x}Ti_{2.5}Al_{10}Fe_{12.5-x}Cu_{10}Ag_5$	70–78				
(at%, x = 0, 2.5, 5)		–	443–460	–	[55]
$Zr_{46}Cu_{37.6}Ag_{8.4}Al_8$	92	–	554	–	[56]
$Zr_{51.9}Cu_{23.3}Ni_{10.5}Al_{4.3}$	102	–	550	–	[56]
$Zr_{51}Ti_5Ni_{10}Cu_{25}Al_9$	100	–	542	–	[56]
$Zr_{62.5}Al_{10}Fe_5Cu_{22.5}$	80	–	459	–	[57]

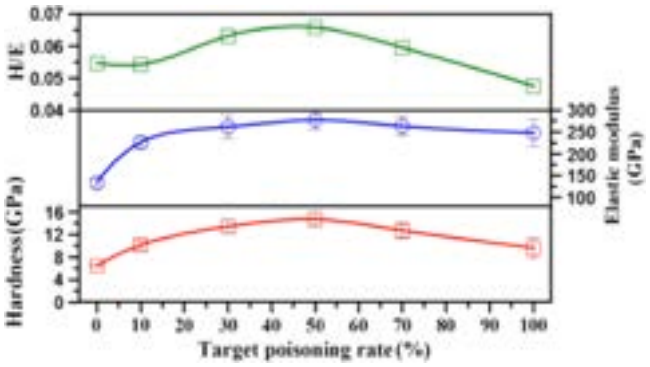

Fig. 5. The hardness, elastic modulus and H/E of Zr–Ni–Al–Si TFMG [42].

The Zr based MGs show pitting behaviour when they are immersed in NaCl [47,70–72]. The Zr-Cu TFMGs develop a passive protective layer of ZrO_2 and display a passive behaviour in the quasi-stationary polarization state in anodic polarization. Additionally, CuO is also formed on the surface by the dissolution of Cu by the hydrolysis reaction[73]. The standard equilibrium potentials are −1.904 V and −0.038 V for Zr/Zr^{4+} and Cu/Cu^{2+}. So the ZrO_2 layer will be formed preferentially compared to CuO [73]. The higher anodic potential passivates the TFMG surface with depletion of copper and enrichment of Zr [74]. Jayaraj et al. [75] and Homazava et al. [76] found the dissolution of copper in polarization curves, and copper tends to dynamically dissolve primary in the 0.5 M NaCl due to the high pitting liability.

4.4. Biological property of Zr-based TFMGs

In the biomedical application, the biomaterials' major requirement is outstanding biocompatibility, which is an essential property that avoids any adverse reaction in the human environment. More biological studies like antibacterial activity, hemocompatibility, in vitro cell line studies and their cell response and in vivo animal studies were employed to inspect the biocompatibility of Zr based TFMGs. Zr based TFMG with Ag and Cu are antibacterial, and the antibacterial activity was studied using the different bacterial strains such as *E. coli* and *S. aureus* [31,45,46,77–79]. The SEM analysis displayed the bacterial cell shrinkage and the death of both bacteria at higher magnification, as shown in Fig. 9D, and the bacterial colony reduction was observed at lower magnification (Fig. 9C) on the Zr based TFMG surface and uncoated surface. The antibacterial behaviour of TFMGs can be attributed to the release of the weakly bonded Cu or Ag ions or redox reaction and chemical ionization [78]. The negatively charged bacterial cell walls attract the metal ions by the electrostatic force of attraction and attach to it, which damages the cell membranes, react with proteins and affect the bacteria and finally killing them [31,77,79].

The material's blood compatibility or hemocompatibility was studied by incubating the specimen with blood. The hemocompatibile surfaces reveal individual RBC without agglomeration and morphology of disc structured biconcave shape, which is the original shape of the blood cells (Fig. 10) on the Zr TFMG surface [63]. The non aggregated platelets with early pseudopodia structure suggest a low initiation of the thrombogenic cycle or no platelet activation, revealing the blood compatibility of TFMG surfaces (Fig. 10), whereas

Table 3
Force created by insertion and retraction of needles, surface roughness and COF of the coatings [61].

Coating material	Insertion peak force (N)		Retraction peak force (N)		Surface roughness (nm)	Coefficient of friction
	Rubber	Pork muscle	Rubber	Pork muscle		
Bare	2.27 ± 0.13	0.15 ± 0.02	1.51 ± 0.05	0.044 ± 0.010	16.2 ± 2.7	0.33 ± 0.03
Ti	2.27 ± 0.18	0.16 ± 0.02	1.64 ± 0.12	0.039 ± 0.006	11.9 ± 1.6	0.36 ± 0.03
TiN	2.06 ± 0.24	0.14 ± 0.02	1.50 ± 0.20	0.034 ± 0.004	14.2 ± 0.7	0.23 ± 0.01
TFMG	0.78 ± 0.09	0.08 ± 0.01	0.43 ± 0.05	0.026 ± 0.003	10.0 ± 1.7	0.05 ± 0.01

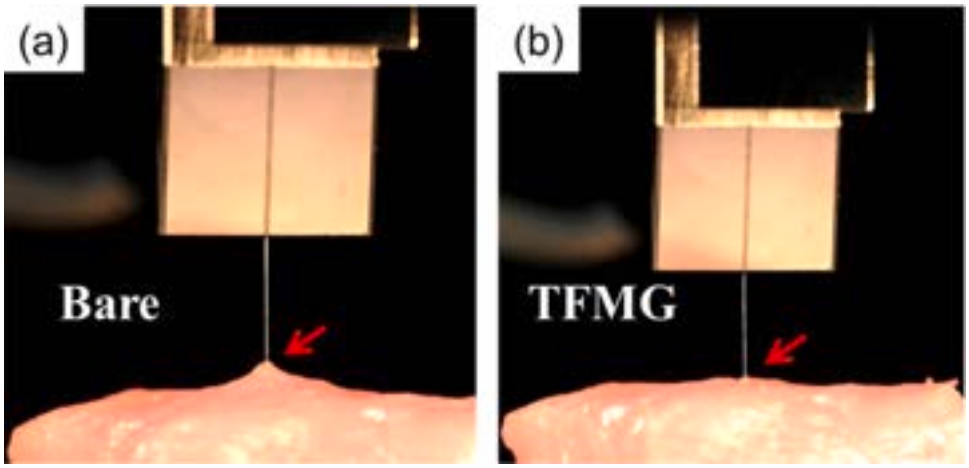

Fig. 6. Images of uncoated needle (a) and TFMG-coated, (b) needles when retracted from pork muscle [61].

the uncoated Ti surfaces are less compatible [63]. The hemocompatibility can also be measured by a Quartz crystal microbalance (QCM) system. The Zr TFMG coated QCM absorbed larger albumin and lower fibrinogen protein, and the TFMG coated QCM attained a lower ratio of fibrinogen/albumin (F/A) was 3.9, which indicates hemocompatibility [80].

Several studies have inspected the cytotoxicity of Zr based TFMG, and the results showed better biocompatibility for TFMG than the uncoated Ti specimens. The in vitro cells line studies like MTT assay and cell morphological studies were carried using mouse fibroblast cells (L929 fibroblast cells) [31,47], mouse preosteoblast MC3T3-E1 cells [46,63,81] etc. The material implanted in the human environment releases metal ionic species, and different biological allergic pathways may be triggered, which cause inflammation and leads to implant loosening and other complications. MTT assay confirms the cell viability and proliferation confirms the nontoxic nature of TFMG. Fig. 11. displays the morphology of the MC3T3-E1 preosteoblast cells cultured on the two systems of TFMGs. A greater number of cells have adhered with red coloured stretched cytoskeleton and blue coloured nuclei spread on the surfaces indicates the viable cells. The elongated cell number, which increases with the period and tremendous growth on the surfaces, indicated the nontoxic nature of TFMGs. Generally, the toxic ions disrupt the structure and the function of cells, which results in distorted morphology of cells, but the cells on the TFMGs retained their original morphology indicating the nontoxic nature [82].

The in vitro studies like cytotoxicity and hemocompatibility are employed to avoid excess animal model usage for non-suitable materials. But the animal model in vivo implant studies only show the actual direct response at the tissue materials interface. Hence, in vivo animal study is required to confirm the material's biocompatibility. The bone formation after 8 weeks of implantation of the new bone formed on the coated specimens is shown in Fig. 12 [63]. The bone formation was good for all three specimens (uncoated Ti, Zr

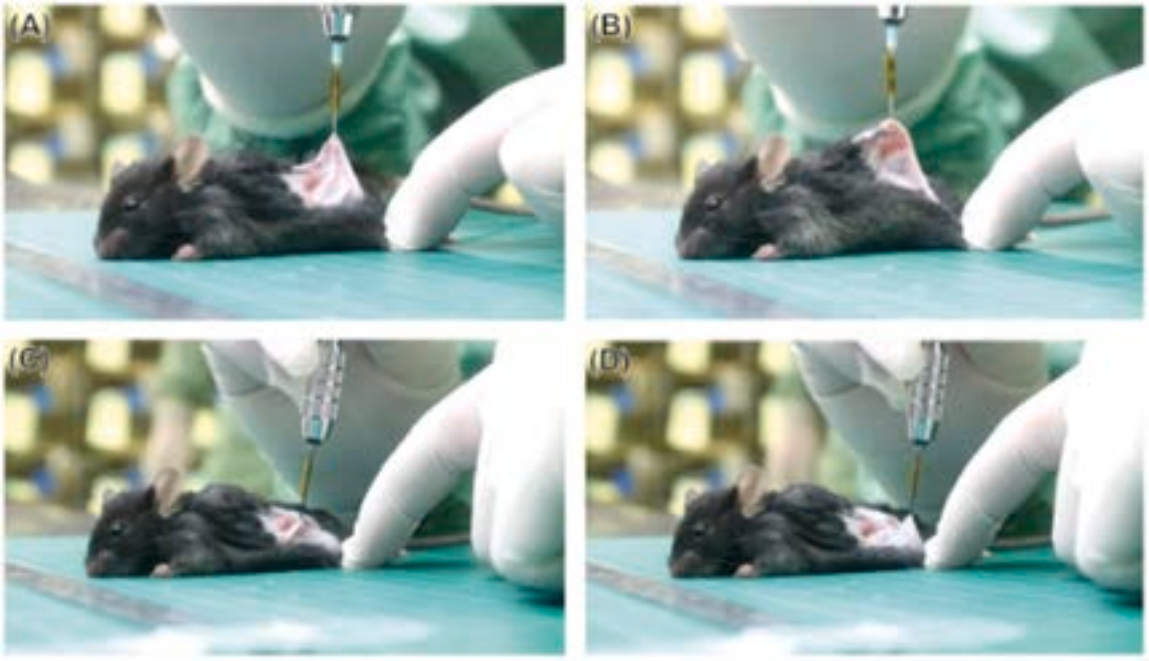

Fig. 7. Photography of puncturing of mouse dorsal skin: (A, B) bare stainless steel needles; (C, D) TFMG-coated needle [62].

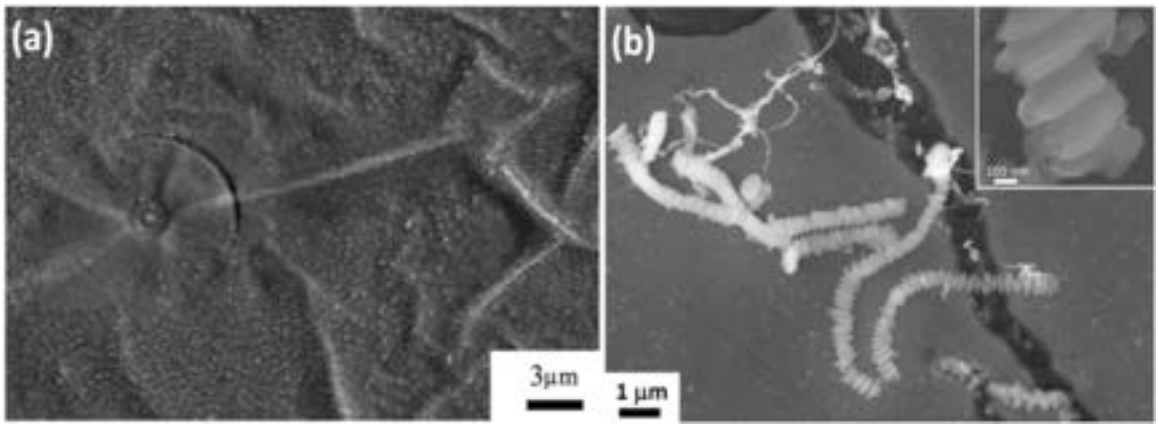

Fig. 8. The morphology of Zr-based TFMGs' after corrosion (a) pit and crevice corrosion (b) the filiform corrosion [67].

TFMG, ZrO_2 thin film) and the bone affinity was greater for control (uncoated Ti) compared to Zr based TFMG [63].

5. Ti-based TFMGs for biomedical implants

Ti-based MGs established quite interesting applications in the biomedical industries because of their ease of fabrication and remarkable mechanical properties like high strength and low Youngs modulus (55–110 GPa), which is nearer to human bone (15–30 GPa) and good in corrosion-resistant property [83]. Although they are good in mechanical property, their composition for glassy metal alloy formation requires the presence of Ni or Be, which are toxic and cause allergic reactions. At present, Ti-based MG's chemical composition eliminate the toxic elements and their enhanced mechanical properties and corrosion-resistant properties makes them extremely feasible for biomedical applications.

5.1. Thermal properties of Ti-based TFMGs

The thermal properties of MGs are more significant due to their role in thermal stability and glassy nature. The DSC parameters of different Ti-based TFMGs have been investigated and displayed in Table 4. When the TFMGs are heated with a constant increase in the rate of heat, the initial stage that occurs is the glass transition temperature (T_g) and later is the crystallization temperature (T_x); the supercooled region ($\Delta T_x = T_x - T_g$) is the region between T_g and T_x. The continuous heating leads to melting temperature (Tm) and liquidus temperature (Tl) crossing the crystallization temperature *(T_x)* [84]. The $Ti_{60}Nb_{15}Zr_{10}Si_{15}$ and $Ti_{40}Cu_{36}Pd_{14}Zr_{10}$ TFMG showed nearly the same and a wide and larger ΔT_x [10,84]. Ti–Cu–Zr–Ni–Hf–Si TFMGs was prepared by Kobata et al. and investigated the thermal formability by varying the bias voltage, and the thermal formability of the TFMGs was enhanced with the increase in bias voltage [85].

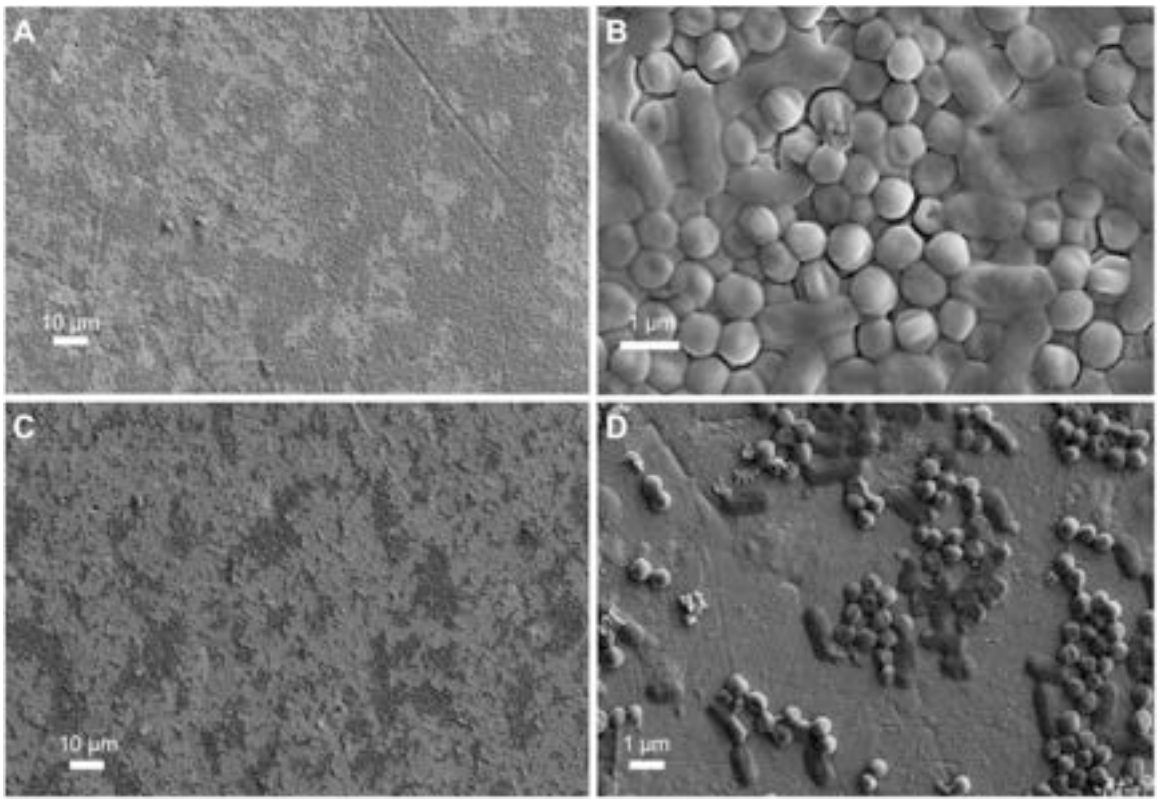

Fig. 9. Bacterial morphology on (A, B) uncoated SS surface and (C, D) Zr based TFMG surface [31].

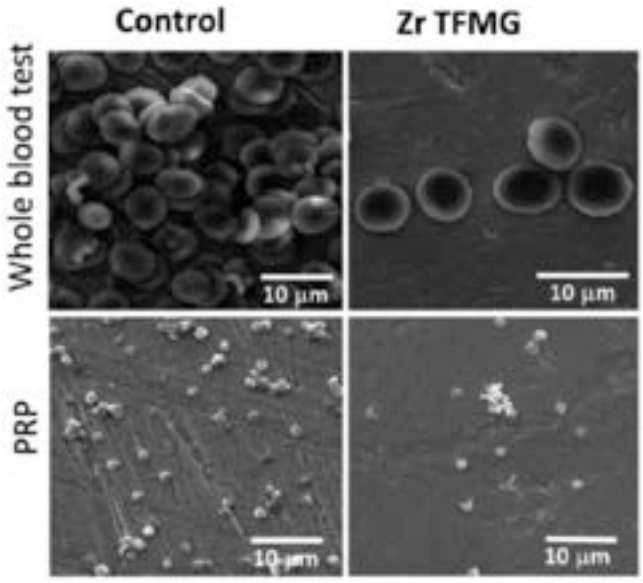

Fig. 10. Hemocompatibility studies of the uncoated Ti and TFMG coated specimen [63].

The increase in bias voltage and the Ar ion bombardment rearranges the film's atoms when grown with Ar incorporation to the glassy structure, and TFMGs thermal stability is improved. The irradiated ions improved the TFMGs ΔT_x, and the amorphous structure and thermal properties are modified [86].

5.2. Mechanical properties of Ti-based TFMGs

The mechanical properties of biomedical materials attain excessive prominence due to their role in biomedical applications. The physical and mechanical properties of the metallic implant materials and Ti and Zr based metallic glasses are compared in Table 5. The Ti-based MGs have comparatively low Youngs modulus, greater fracture strength, outstanding specific strength and good compressive yield strength.

Nanoindentation is a reliable and convenient way to evaluate the TFMGs' mechanical properties like Young's modulus and hardness gained from a solo test. The summary of the mechanical properties of Ti-based TFMGs and BMGs are displayed in Table 6. The measured Young's modulus and hardness are greater than the BMGs, which may be due to the difference in the microstructure between the as-sputtered film and the bulk counterpart. Fig. 13 displayed a typical load vs indentation curve obtained for Ti-based TFMG. Two systems of Ti-based TFMG showed Youngs modulus of 110 GPa [91]and 106.4 GPa with a hardness of 7 GPa [91,92].

The scratch test evaluates the scratch resistance and adhesion of the coatings to the substrate. The thin film's adhesion failure at normal load is evaluated by the critical load (Lc), which indicates resistance to scratch. When the Lc is higher, the applied force is also higher to make a scratch on the film, which implies the coating is more resistant to scratch. The Lc1 indicates the initial crack occurrence, Lc2 (first delamination) is due to local interfacial spallation or fragmenting failure and Lc3 (total delamination) is the total damage of coating [52]. The Ti-Cu-Pd-Zr TFMG showed an Lc3 of 2.53 ± 0.558 N and the work of adhesion was calculated from the formula [91]:

$$Lc = \frac{\pi d_c^2}{8}\sqrt{\frac{2EW}{t}} \quad (1)$$

where,

Lc - critical load
d_c - track width
E - coatings' elastic modulus
T- thickness of the film
W - work of adhesion

The work of adhesion of the film was calculated for the critical loads Lc3 is 1.4×10^{14} N/m [91].

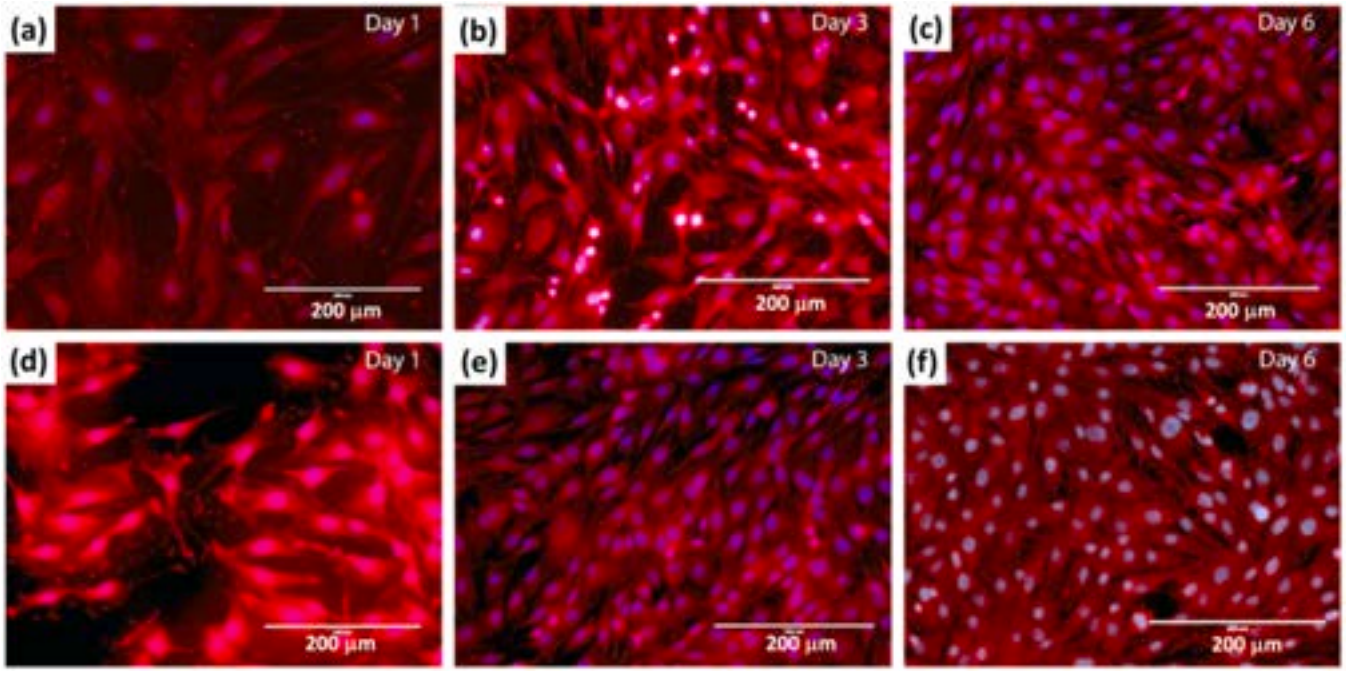

Fig. 11. The MC3T3-E1 cell morphologies (a–c) Zr-Ti-Cu-Ag and (d–f) Zr-Ti-Co-Ni TFMGs for different period of time [82].

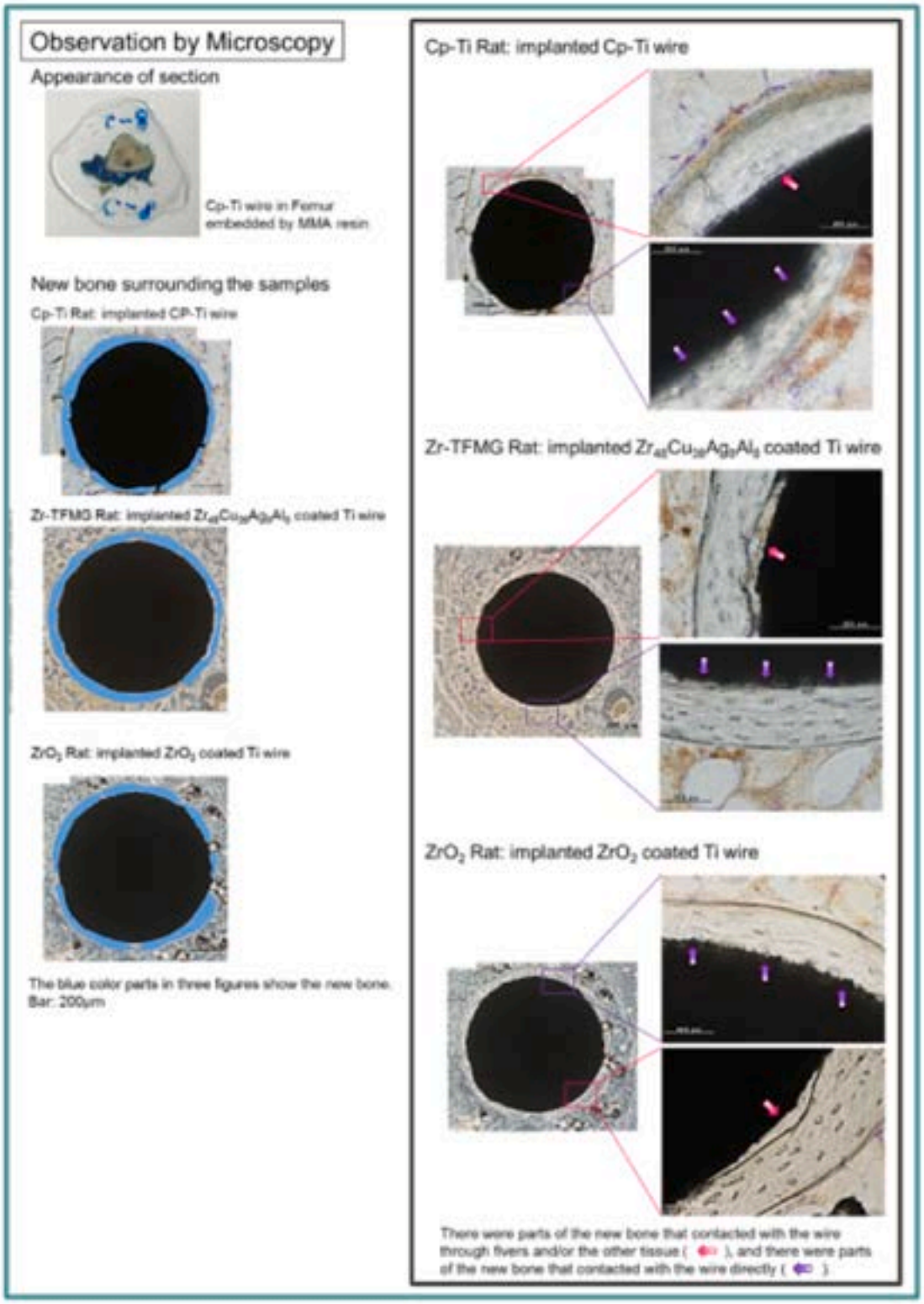

Fig. 12. Microscopic images of the specimen implanted bone after 8 weeks [63].

5.3. Corrosion properties of Ti-based TFMGs

The chemical stability and environmental stability of the TFMG can be assessed by the corrosion studies based on the electrochemical reactions. Corrosion studies of Ti-based TFMGs have been carried out by the researchers in different types of electrolytes such as simulated body fluid (SBF) [10,91,92], Hank's solution [64,100], 1 mass% Lactic acid [101], phosphate buffered saline (PBS) [101,102], HBSS [101] and Ringer solution [103]. The electrochemical reaction of the Ti based TFMGs in SBF with different contents of titanium was measured by Ke et al. [64]. The corrosion resistance becomes progressively higher when titanium content increased in the film [64].

Table 4
The DSC parameters of Ti based TFMGs.

Material	T_g	T_x	ΔT_x	Reference
$Ti_{24}Ni_{55}Zr_{21}$	736 K	789 K	53 K	[87]
$Ti_{38}Ni_{49}Zr_{13}$	–	754 K	–	[87]
$Ti_{40}Cu_{36}Pd_{14}Zr_{10}$	508.1 °C	557.4 °C	49.3 °C	[84]
$Ti_{60}Nb_{15}Zr_{10}Si_{15}$	451.3 °C	506.3 °C	51 °C	[10]
$Ti_{65}Si_{15}Ta_{10}Zr_{10}$	464 °C	515 °C	51 °C	[88]
$Ti_{45}Cu_{35}Zr_{20}$	331 °C	374 °C	43 °C	[88]
$Ti_{57}Cu_{28}(Zr_{0.95}\text{-}Hf_{0.05})_5Si_{10}$	587 °C	601 °C	–	[89]
$Ti_{41.5}Cu_{42.5}Zr_{2.5}Ni_{7.5}Hf_5Si_1$	702 K	747 K	45 K	[85]

Fig. 14. shows the potentiodynamic polarization plots (Tafel) and impedance of the TFMG and uncoated Ti. The nobler potential and the higher Rct of TFMG showed corrosion resistance behaviour with very little corrosion rate [92].

When the coated samples were placed in the electrolyte, a passive layer is formed, and the Ti oxidise forms a layer of TiO_2 which is the reason for nobler potential and resistance to corrosion. The Ti-based TFMGs displayed passive behaviour with a minimum corrosion rate compared to conventional biomedical alloys such as 316L SS [91], Ti and its alloys[10,92].

5.4. Biocompatibility of Ti-based TFMGs

The biocompatibility of the TFMG materials used as implants attains great importance. These implant materials should have the ability to co-exist in the human body interacting with tissues and without producing any adverse reaction. Biological studies like antibacterial activity, hemocompatibility, in vitro cell line studies and their cell response and in vivo animal studies can be employed to inspect the biocompatibility of Ti-based TFMGs. Ti-based TFMG with Cu are antibacterial, and the antibacterial activity was studied using the different bacterial stains such as *E.coli* (Fig. 15) [91]. The SEM images (Fig. 15(I)) show the reduction of bacterial colonies and the cell density on the TFMG coated specimen at lower magnification. The higher magnification displays shrunk or distorted bacterial cells. The *E.coli* destruction was visualized by Epi-fluorescent microscopy images (Fig. 15(II)) in wet condition. Initially, *E.coli* was green, and they were alive; after 12 h of incubation with TFMG, they turn red in colour, confirming the bacterial death. The antibacterial activity may be due to the presence of copper in the alloy. When the copper is in contact with the bacteria, it will weaken the cell membrane, and holes will be created through which copper ions enter the cell and damage the entire system [91].

Hemocompatibility is a necessary factor for biocompatibility which replicates the grade of an interface between material and blood. The SEM images (Fig. 16.) represents the uncoated Ti and Ti-based TFMG coated specimens employed for hemocompatible studies with blood cells [10]. The bare substrate showed the morphology of accumulated and activated platelets with 3D fibrin mesh formation leading to the RBCs agglomerations and platelets deformation and finally the thrombus formation. The coated specimen exposed no cluster formation of RBCs and maintained a biconcave shape, which is the RBCs' original morphology without agglomeration representing better blood compatibility [10].

The biocompatibility and bioactivity of the Ti-based TFMGs have been examined via both in vitro cell response (cytotoxicity and mineralization) and in vivo animal studies. The cytotoxicity studies studied for Ti-based TFMGs, and outcomes have validated that Ti-based TMGs exposed better biocompatibility than uncoated Ti specimens. The in vitro cell line studies like MTT assay and cell morphological studies were carried using mouse fibroblast (L929 fibroblast cells) [10,31,84], mouse pre-osteoblast MC3T3-E1 cells [10],osteoblast SaOS2 cells [10,104], MG-63 cells [105]. The in vitro cytotoxicity studies of Ti based TFMG by L929 fibroblast cells are shown in Fig. 17. The cells grown in the TFMG extracts are observed to have distinct stress fibres and elongated morphology even in 100% concentration of extracts, confirming the viable cells and nontoxic nature of Ti-based TFMG [92].

The osteoblast cells should adhere to the TFMG surface, which influences the proliferation and differentiation. The SaOS-2 cells

Table 5
The mechanical properties of several implant materials and bone [90].

Properties	Natural bone	Ti alloy	Co-Cr alloy	Stainless steel	Ti-based MG	Zr-based MG
Density (g/cm^3)	1.8–2.1	4.4–4.5	8.3–9.2	7.9–8.1	4.4–5.2	5.9–6.7
Young's modulus (GPa)	3–20	110–117	230	189–205	78–115	80–100
Compressive yield strength (MPa)	130–180	758–1117	450–1000	170–310	1950–2165	~200
Fracture toughness ($MPa\,m^{1/2}$)	3–6	55–115	N/A	50–200	40–100	50–90

Table 6
Summary of Ti-based TFMG and BMG systems and their mechanical properties.

Chemical composition (at%)	Youngs modulus GPa	Hardness GPa	Vickers hardness (Hv) ($kg\,mm^2$)	Specific strength (kN m/kg)	Reference
TFMGs					
$Ti_{40}Cu_{36}Pd_{14}Zr_{10}$	106.4	7	–	–	[92]
$Ti_{47}Zr_{41}Si_{12}$	109	5.2	–	–	[64]
$Ti_{58}Zr_{33}Si_9$	115	5.3	–	–	[64]
$Ti_{66}Zr_{25}Si_9$	116	6.2	–	–	[64]
$Ti_{75}Zr_{19}Si_6$	110	4.8	–	–	[64]
$Ti_{40.8}Cu_{42.3}Zr_{2.5}Ni_{7.3}Hf_{4.7}Si_1O_{1.4}$	128	6.5	–	–	[86]
BMGs					
$Ti_{40}Cu_{36}Pd_{14}Zr_{10}$	82	–	–	270	[93]
$Ti_{45}Zr_{10}Cu_{31}Pd_{10}Sn_4$	95	–	650	–	[94]
$(Ti_{0.45}Zr_{0.1}Pd_{0.1}Cu_{0.31}Sn_{0.4})$ 100-xMx (M: Ta and Nb) (x = 1–5)	97–119	–	–	–	[95]
$Ti_{20}Zr_{20}Ni_{20}Cu_{20}Be_{20}$	130	8	–	–	[96]
$Ti_{20}Zr_{20}Hf_{20}Cu_{20}Be_{20}$	125	7.6	–	–	[96]
$(Ti_{45}Cu_{40}Zr_{10}N_{i5})100 - xAl_x$ (x = 0–8)	60–160	5.5–7.3	–	–	[97]
$Ti_{41.5}Zr_{2.5}Hf_5Cu_{37.5}Ni_{7.5}Si_1Sn_5$	150	4.7	600	–	[98]
$Ti_{40}Zr_{25}Ni_{12}Cu_3Be_{20}$	95	–	530	–	[56]
$Ti_{47}Cu_{38}Zr_{7.5}Fe_{2.5}Sn_2Si_1Ag_2$	100	–	588	–	[99]

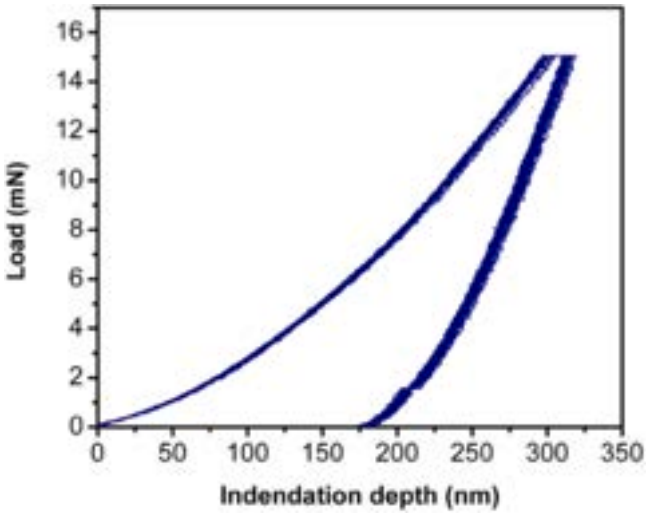

Fig. 13. Load vs indentation curve obtained for Ti based TFMG [92].

were used for differentiation and mineralization for Ti-based TFMG by Rajan et al. The studies carried out confirm uniform coverage of SaOS-2 cells, similar to TCPS control (Fig. 18). The alkaline phosphatase (ALP) activity of the SaOS-2 cells was greater than uncoated TiAlV (control) and also showed good mineralization (calcification) [10]. MC3T3-E1 cells were cultured on Ti-based TFMG and stained with the alizarin red s, and the crimson red colour on the samples confirms the calcium deposits [10].

In vivo studies of Ti-based TFMG extracts were carried out on Albino rabbits by Rajan et al. The studies confirmed no erythema and oedema formation and did not display any indications of toxicity. The index of irritation for erythema and oedema was zero for control, and for specimen extract, it is 0.03 for all animals (rabbits), which is an indication of nontoxicity [10].

6. Fe-based TFMGs for bioimplants and devices

Compared to Zr-based or Ti-based MGs, Fe-based MGs are very much lower in cost, making them economically feasible for bioimplants applications on a large scale and having a good GFA. Fe based MGs are attractive due to their very high fracture strength, excellent hardness and superior resistance to corrosion and magnetic properties [106].

6.1. Thermal properties of Fe-based TFMGs

TFMG systems are based on the empirical rules set forwarded by Inoue. (1) MGs should have a minimum of three elements, (2) they should have a mismatch of atomic size above 12% and (3) they should have a negative heat of mixing for the main components [107]. The heat of mixing of atomic pairs of Fe based alloy is displayed in Table 7.

Chen et al. studied five Fe based TFMGs with different Fe content. When the Fe content increases in the composition, the T_x increases from 909.4 K to 989.2 K, but the SCLR ΔT is not dependent on Fe concentrations. The highest ΔT is for lowest Fe containing TFMG with 37.6 wt% while the highest Fe composition showed a lower ΔT of 26.3 °C [108]. Fe-Cr-Mo-C-B-Y MGs of two different forms (rod and film) were employed for DSC. The MG in rod form showed T_g and T_x, whereas no T_g was found for the TFMG. The volume fraction of the amorphous phase in a TFMG calculated by comparing ΔH (heat of crystallization) of the TFMG using the below formulae, and for rod, was found as 89.7% [109].

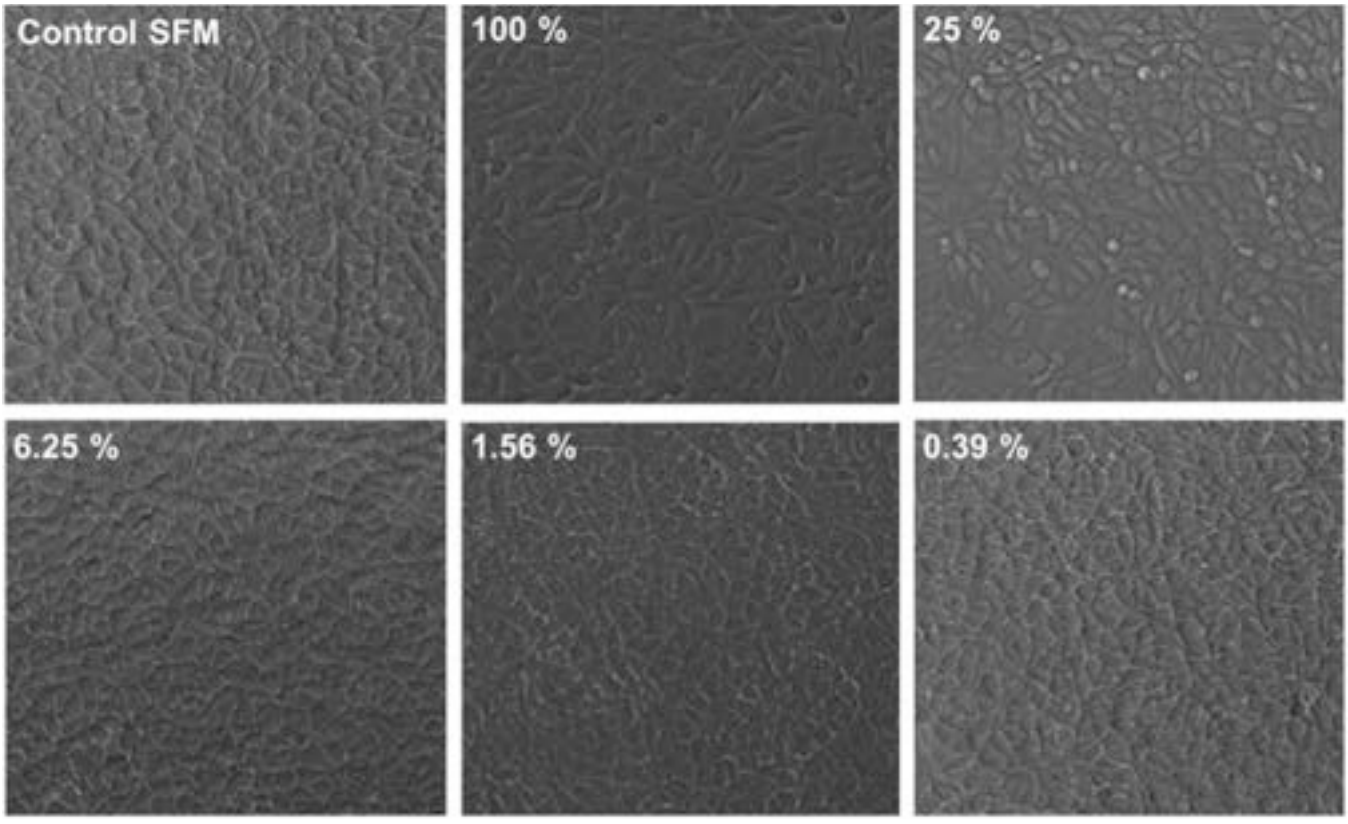

Fig. 14. (a) Tafel plot and (b) AC impedance studies of TFMG coated and uncoated Ti [92].

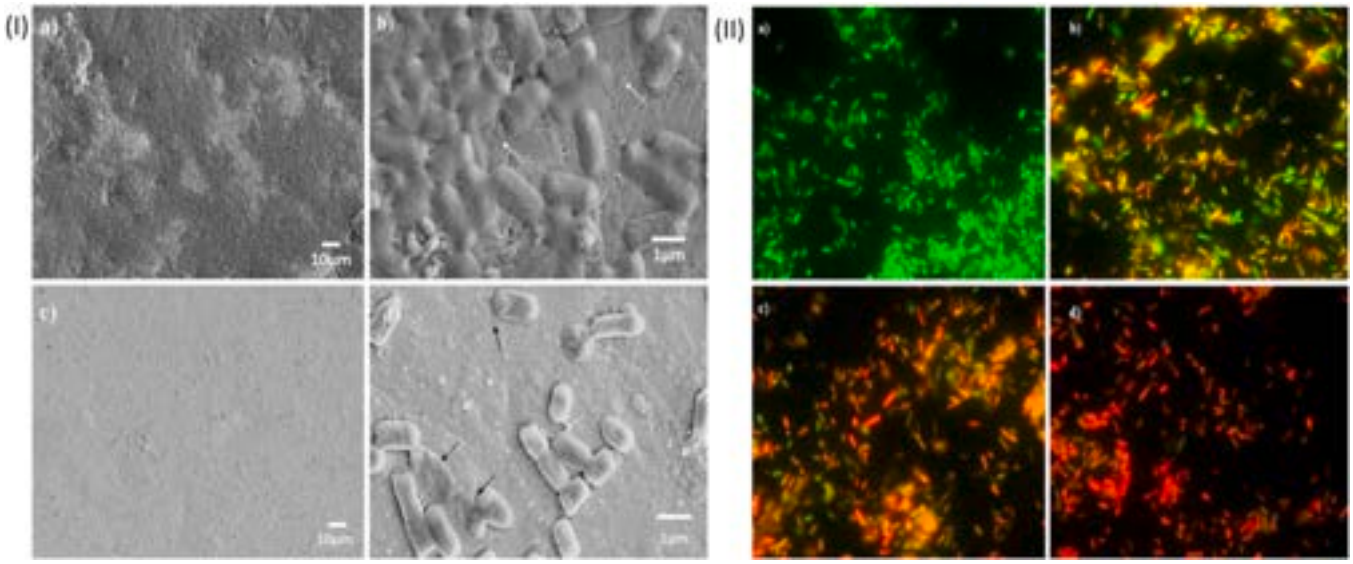

Fig. 15. (I) The bacterial morphology on (a, b) uncoated SS and (c, d) Ti based TFMG surface, (II) Epi-fluorescent microscopic images of E. coli: (a) initial, (b) 4 h, (c) 8 h, (d) 12 h [91].

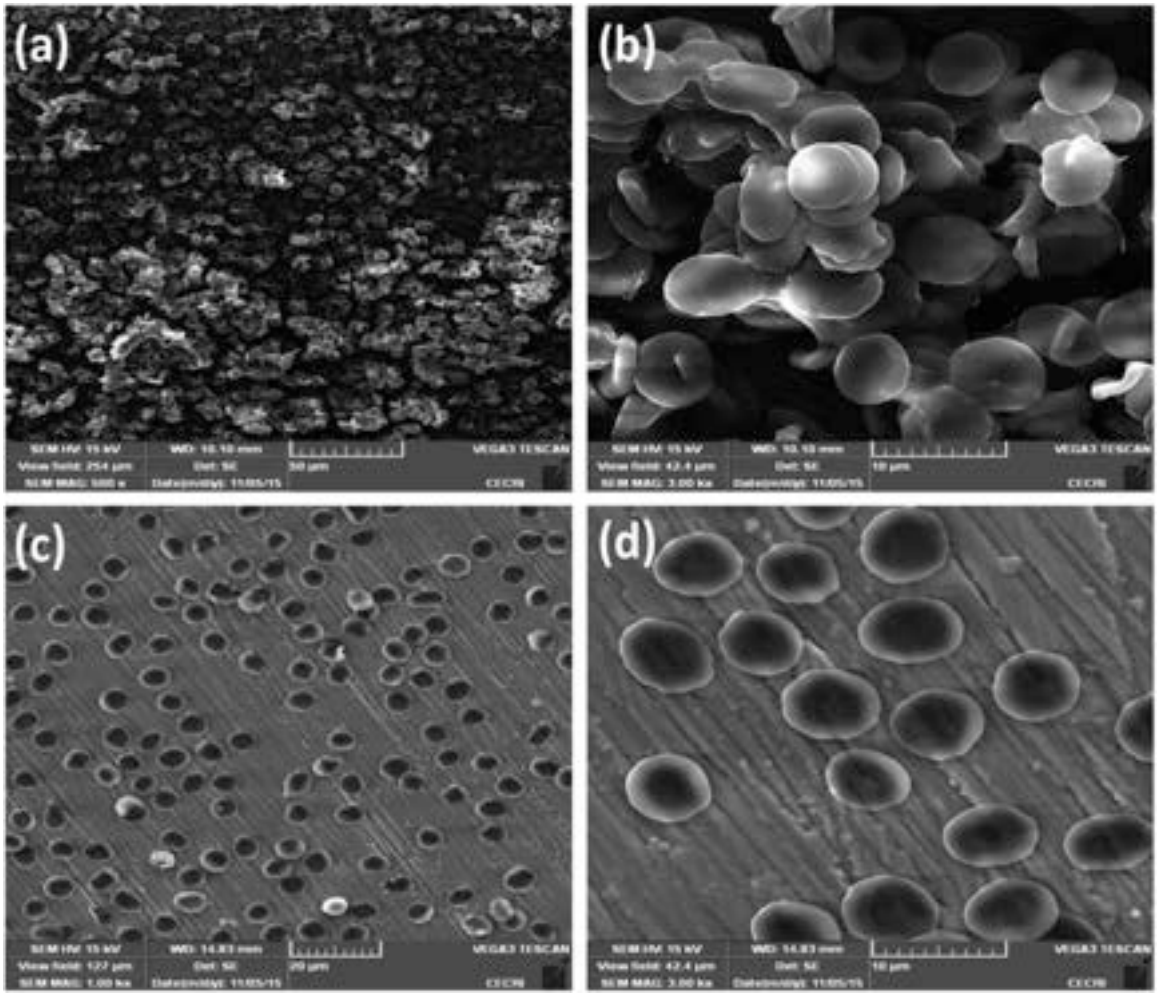

Fig. 16. SEM analysis after the blood contact (a, b), uncoated Ti (control) lower magnification and higher magnification (c, d), Ti based TFMG lower magnification and higher magnification [10].

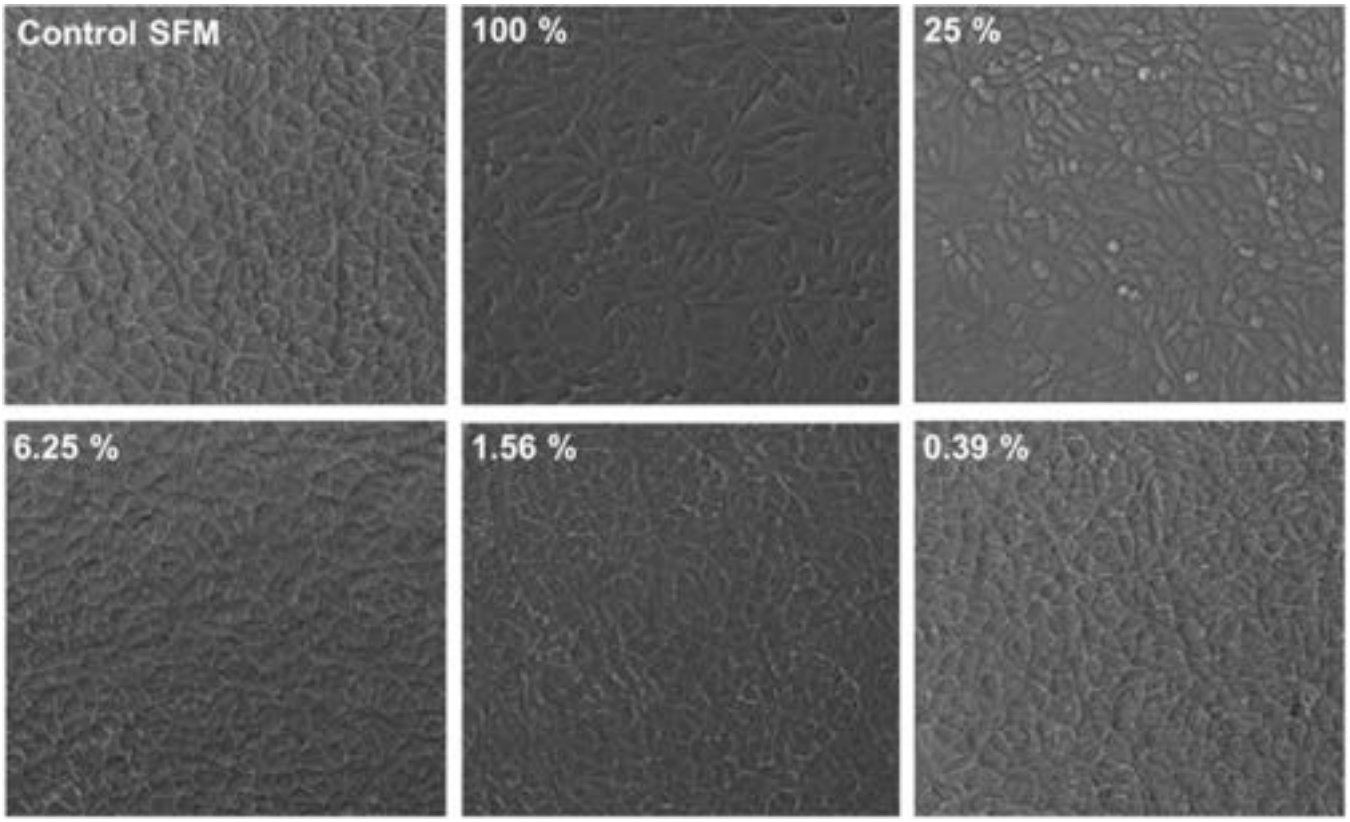

Fig. 17. Microscopic images of L929 cells in different TFMG extract concentrations [92].

$$am.\ \% = \frac{\Delta H_{coating}}{\Delta H_{rod}} \quad (2)$$

When a rare earth element is added to the Fe-B-Nb system, the ΔT (SCLR) will increase rapidly. The TFMG with Nd showed greater ΔT and higher glass-forming ability [110]. Fe-B-Nd-Nb TFMG showed a ΔT of 96 K. The reason for higher SCLR can be attributed to the substrate's strain acting in the TFMG, which controls the annealing [111].

6.2. Mechanical properties of Fe-based TFMGs

Nanoindentation is an appropriate approach for evaluating the mechanical properties such as the film hardness and modulus experimentally. The summary of the mechanical properties of Fe based TFMGs and BMGs are displayed in Table 8.

Fig. 19a. exhibits a characteristic load-displacement curve including loading, holding and unloading from which Young's modulus and hardness information can be obtained. The hardness, elastic modulus and H/E ratio of Fe-Zr-Ti TFMGs with different Fe content are displayed in Fig. 19b. When the Fe concentration increases hardness, elastic modulus and H/E ratio increase proportionally [108]. Fig. 19a. portrays the load-displacement curves of Fe-Zr-Ti TFMGs with different Fe content showing clear, discrete pop-ins. The pop-ins are related to a single shear band and quickly accommodate the applied strain, leading to a load drop. The breakage of displacement is due to the activation of a shear band in the course of nanoindentation [108]. Similar observations of pop-ins are found in Fe-Cr-Mo-Co-C-B-Si TFMGs fabricated at different sputtering currents [113]. By tuning the TFMG compositions, the mechanical properties of Fe-based TFMGs' can be improved.

Surgical blades' sharpness was evaluated by blade sharpness index (BSI). BSI is the ratio of external load applied to work done to the necessary energy needed to propagate a cut in the material. The BSI can be calculated from the formula [106]:

$$BSI = \frac{\int_0^{\delta i} F dx}{\delta_i t J_{Ic}} \quad (3)$$

Where,

F- applied force,
dx - increment of blade displacement,
δ_i - initial depth of blade indentation before substrate fracture
t - thickness of substrate
J_{Ic} - resistance to fracture.

Jang et al. studied the sharpness of the commercial blade, and TFMG coated SS blade revealed a TFMG blade showed lower BSI (0.28) compared to the uncoated SS blade (0.31), which corresponds to sharpness improvement on coated blades. The TFMG coated blade was more durable even at 50 cm cutting length may be due to its greater hardness of 1200 HV [106]. Adhesion of the Fe-Zr-Nb TFMGs of different Nb content was studied Lou et al. by scratch test and HRC-DB test. The Daimler-Benz Rockwell-C (HRC-DB) adhesion test uses an extreme load of 1471 N to assess the bonding of TFMGs with the substrate. All the TFMGs showed good adhesion property ranging from 39.9 N to 50 N, but Fe-TFMG with lower Nb content showed excellent adhesion property. HRC-DB test revealed excellent adhesion of HF1. The scale of HF1 to HF4 are good quality of adhesion of films to the substrates [117].

6.3. Corrosion of Fe-based TFMGs

The stainless steel of biomedical grade releases Ni ions when used as an implant for a long term in the aggressive biological environment. The Fe base TFMG coated on SS showed greater pitting

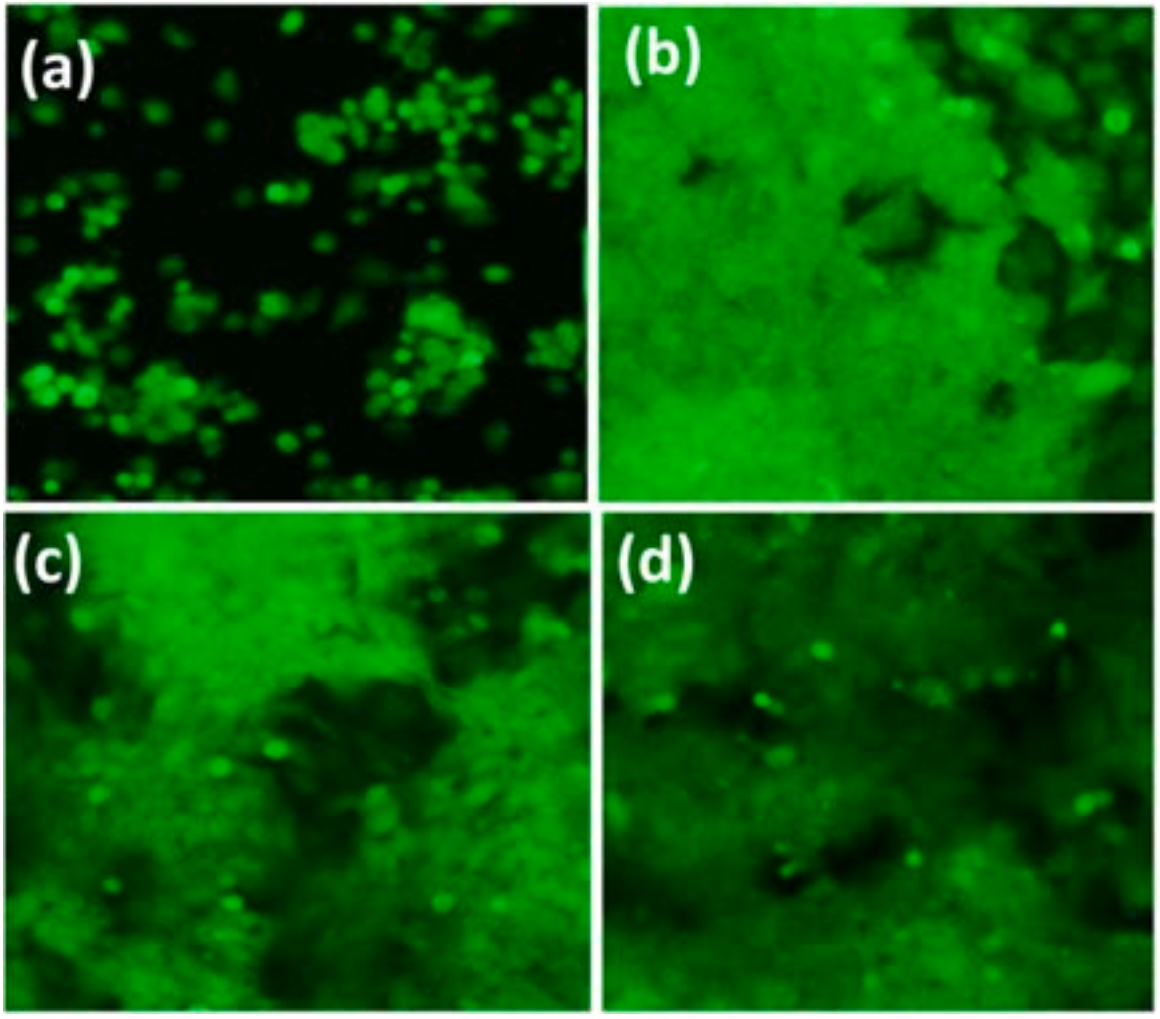

Fig. 18. Microscopic images of the growth of SaOS-2 cells (a) Ti6Al4V, (b)TFMG, (c)TCPS undifferentiated control, (d) TCPS differentiated control [10].

Table 7
The heat of mixing of atomic pairs [108].

Atomic pair	Heat of mixing, ΔH_{mix} (kJ/mol)
Fe–Zr	25
Fe–Ti	−17
Zr–Ti	0

potential and lowered passivation current density in artificial sweat solution. After pitting corrosion, the TFMG exposes a very sluggish upsurge in the current density, which is attributed to the formation of a passive layer or by-product layer of corrosion [118]. Corrosion studies of Fe based TFMGs have been carried out by the researchers in different types of electrolytic solution like artificial sweat solution [118] Ringer's solution [117] Hank's solution [119], 5 wt% NaCl aqueous solutions [108,113] and 1 K mol/m^3 HCl aqueous solution [109]. The stainless steel (AISI420) resistance to corrosion was enhanced from 12 to 65 times greater by coating Fe based TFMG on to it in ringer solution [105,117]. The uncoated SS surface showed corrosion pits and by-products due to corrosion. But the TFMG coated surfaces are without any defects like holes showing the influence of Nb addition on the enhancement of corrosion resistance of the TFMG

Table 8
Summary of Fe-based TFMG and BMG systems and their mechanical properties.

Chemical composition (at%)	Youngs modulus GPa	Hardness GPa	Vickers hardness (Hv) (kg mm^2)	Specific strength (kN m/kg)	Reference
TFMGs					
Fe_{37-33} Zr_{35} Nb_{21-26}	107–114	8–8.6	–	–	[112]
Zr_{38-29} $Ti_{21\ to\ -17}Fe_{37-49}$	102–124	7.3–9.3	–	–	[108]
$Fe_{44}Cr_{15}Mo_{14}Co_7C_{10}B_5Si_5$	193.4	8.45	–	–	[113]
BMGs					
$Fe_{63}Mo_{14}C_{15}B_6Er_2$	204	–	1122	–	[114]
$Fe_{55}Cr_8Mo_{14}C_{15}B_6Er_2$	209	–	1122	–	[114]
$Fe_{48}Cr_{15}Mo_{14}C_{15}B_6Er_2$	213		1122		[114]
$Fe_{49}Cr_{15}Mo_{14}C(13+x)B(8\text{-}x)Er_1$ (x = 2, 4, 5 and 6)	210–220	–	–	–	[115]
$(Fe_{0.9}Co_{0.1})_{58.5}Cr_6Mo_{14}C_{(15+x)}$ $B_{(6-x)}Er_{0.5}$ (x = 3 and 4)	200	–	–	–	[115]
$Fe_{70}B_{20}Si_{10}$	–	–	714	–	[54
Fe_x (x = 63–71) Cr_y (y = 0–3)Moz(z = 5–12) $P_{12}C_{10}B_2$	176–183	–	845–974	–	[116]

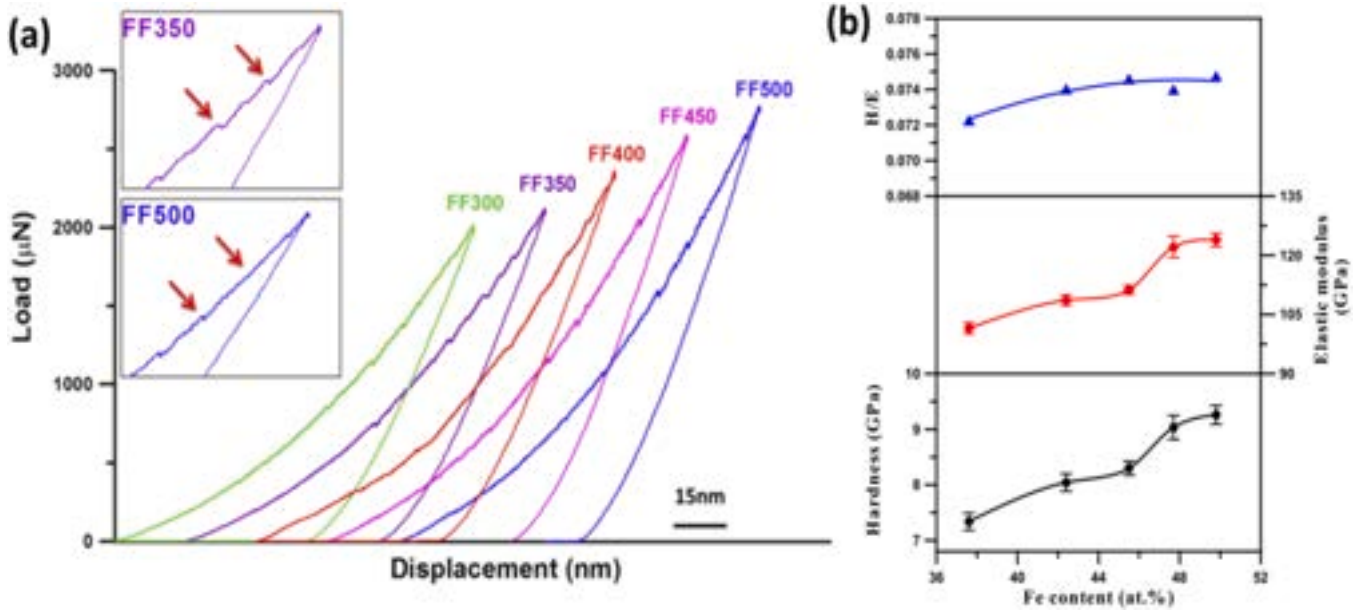

Fig. 19. (a) Nanoindentation load-displacement curves and (b) The hardness, elastic modulus and H/E ratio of Fe–Zr–Ti TFMGs with different Fe content [108].

[117]. Similarly, the AISI420 SS substrate was coated with Fe-Zr-Ti TFMG with different Fe concentrations by Chen et al. who studied their corrosion behaviour [108]. The greater corrosion resistance of the amorphous TFMGs is due to the irregular atomic arrangement, absence of dislocation, vacancy and absence of crystalline defects. The resistance to corrosion can be improved by alloying components having strong passivation capabilities like Ti, Cr, Mo and the valve elements such as Al, Zr, Hf, Nb and Ta [120]. The different atomic size reduces the free volume, and the vacancy and voids are prevented in TFMG which is also a reason for the improved anticorrosion property.

6.4. Biocompatibility of Fe-based TFMGs

The improved mechanical and corrosion property assure the biocompatibility of Fe-based TFMGs as forthcoming biomaterials. The necessary requirement of a material used on the tissues is its capability to avoid any contrary effect. The reports say the Fe-based TFMGs displayed enhanced biocompatibility for in vitro cells line studies such as for MG-63 cells [105,117], L929 and NIH3T3 fibroblast cell [119]. MTT assay showed more viable cells for L929 and NIH3T3 cell lines compared to the negative control. The L929 cell density increases in a culture period of four days and the morphology of the cells in later periods seem to be spindle-shaped and elongated morphology [119]. The osteosarcoma MG63 cell line was adopted to study the toxicity of the TFMG [117]. The coated specimen exposed noteworthy O.D. (optical density) value for the fifth day, and the Fe-Zr-Nb coatings provided a better cell growth and viability, which is free of toxicity and demonstrates their enhanced biocompatibility [117]. The metallic ions of Fe and Nb in allowed concentrations are less toxic, and a trace amount of Fe (metallic part of haemoglobin) is present in human blood [117,119].

7. Biodegradable metallic glasses

Compared with traditional bioinert materials, biodegradable temporary implants are more desirable in the biomedical field as these biodegradable materials gradually dissolve and are consumed

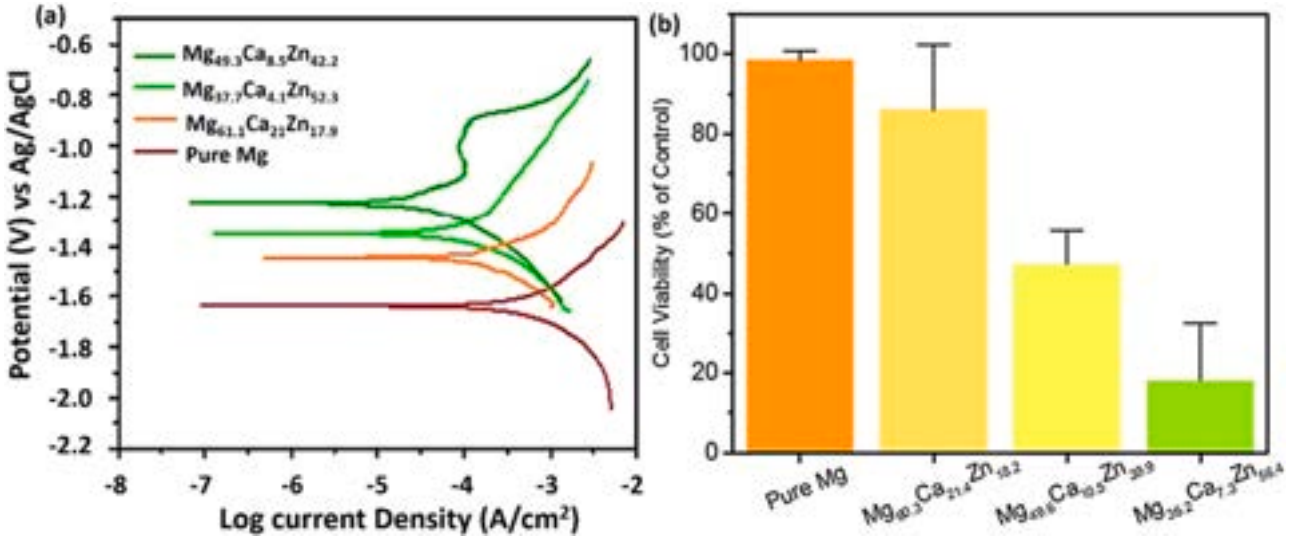

Fig. 20. (a) Tafel plot of Mg based TFMG and pure Mg (b) MTT cell viability of MG63 osteosarcoma cells [132].

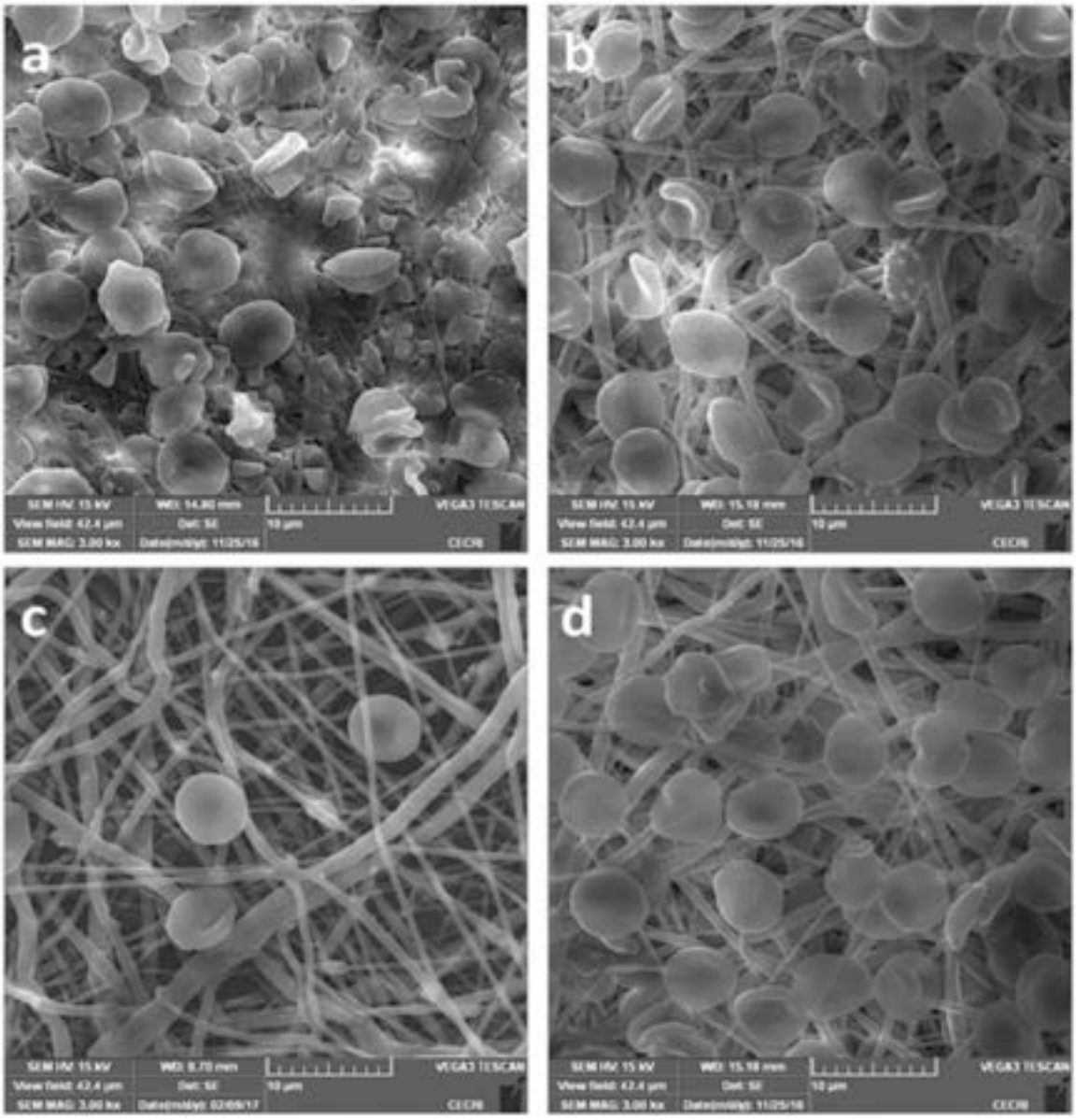

Fig. 21. SEM analysis after the blood contact (a) PCL, (b) PCL/Mg TFMG, (c) PCL/HA, (d) PCL/HA/Mg TFMG [133].

in the body environment and thereby eliminate the necessity for removal surgery of the implant after healing [121]. In the arena of degradable implants, Mg and its alloys are most interesting as a non-toxic, biodegradable and bioabsorbable material [122]. The evolution of hydrogen is efficiently suppressed in vivo with no impact on biocompatibility, and the degraded product ions stay well in humans [15]. Mg-based MGs exhibit lower Young's modulus (20–30 GPa), which is almost comparable with the human bones and a density of about 1.6–2.4 g/cm^3; these properties make them potential applicants as biomedical materials [123].

The progress of magnesium faces some practical challenges. The magnesium and Mg alloys' rate of degradation is higher in the human body environment, which result in the fall of mechanical integrity of the Mg implant before the healing time ends for the bone tissues. Two different methods can reduce the corrosion or degradation of Mg. The primary one is alloying the biocompatible elements with Mg. The second one is modifying the material by any treatment or coating a protective layer over it that delivers a resistive barrier to corrosion in the body environment.

The ternary Mg-Zn-Ca MGs have gained attention with improved corrosion resistance and lightweight in biomedical applications [124–126]. Mg forms $Mg(OH)_2$, which is more active in improving embryonic cell growth, and it is also antibacterial. The Ca addition in the alloy forms fine Mg_2Ca precipitates and improves the mechanical property by precipitation hardening [127,128]. The tensile strength and creep strength is improved with Zn addition, and also they decrease grain size and enhance the alloy castability [129]. It is reported that the solubility of Zn was 2 wt% into Mg at room temperature in the equilibrium state. When the Ca and Zn are in appropriate amounts in the Mg-Zn-Ca MGs system, they exhibit a greater combination of resistance to corrosion and mechanical properties with biocompatibility. Different elemental composition and fabrication techniques were employed to fabricate fully amorphous Mg-based MGs with minor difficulties and cost effectiveness [130].

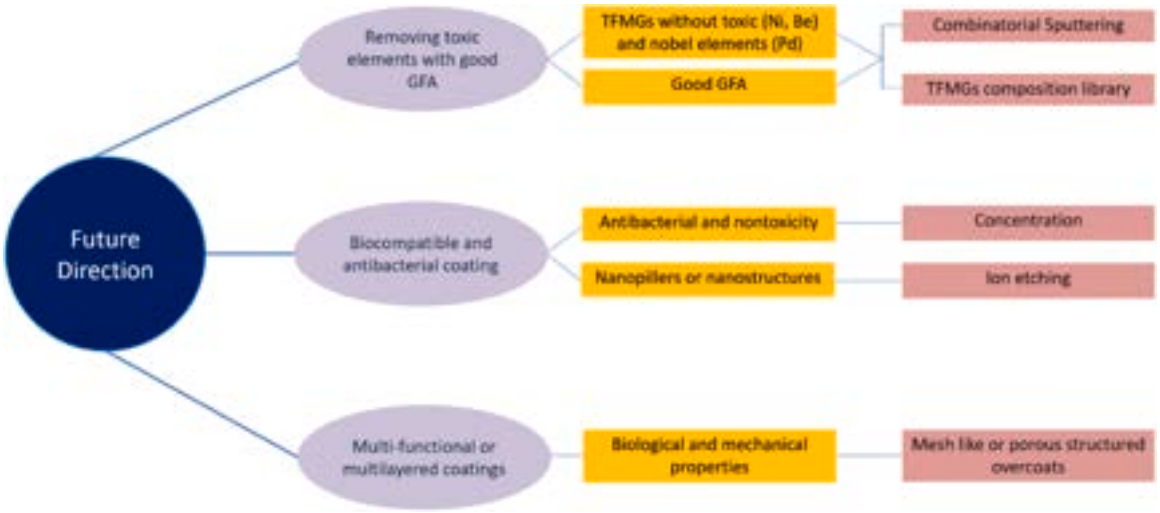

Fig. 22. Representation of various challenges encountered by TFMGs and its future research direction. The extreme right column recommends further research investigation of TFMGs.

7.1. Mg based TFMG

Mg based TFMGs have currently dragged in huge attention due to their encouraging biocompatibility, biodegradability and mechanical properties. Only a few research pieces are going on Mg TFMG and little used for biomedical application because of the degrading property. The Mg-based TFMG can be fabricated by pulsed laser deposition (PLD) [131] and Sputtering [123,132,133]. Liu et al. fabricated Mg-Zn-Ca TFMGs of different thickness, and the found the density of the film decreases with increase in thickness and the grain size remains unchanged [123]. The corrosion characteristics and biocompatibility of Mg TFMGs of different composition of Zn were studied by Li et al. [132]. The TFMGs showed good corrosion resistance compared to pure crystalline Mg, and when the zinc content got increased to more than 50%, it showed passivation (Fig. 20a). The cell viability of human osteosarcoma cells (MG63) was reduced when the Zn content increased and the cell attachment and proliferation also showed that an increasing Zn content hindered the cell proliferation and resulted in poor biocompatibility (Fig. 20b) [132].

Biodegradable polycaprolactone (PCL) with nano-hydroxyapatite was electrospun, and Mg TFMG was coated on electrospun fibres. The MG TFMG coated scaffolds showed (Fig. 21.) the disc structured biconcave shape for the attached RBCs representing better blood compatibility [133].

8. Future perspective and challenges

Although BMGs have great potential as future biomaterials, there are considerable challenges associated with the development of biomedical BMGs. The limited critical sizes of BMGs would hinder the design of biomedical devices with complicated shapes using BMGs. Besides, structural relaxation and the associated embrittlement may occur in some BMG systems while processing via annealing treatments. Here, the key issues faced by TFMGs, some proposed strategies and future research trends are briefly described. Fig. 22 illustrates the current challenges faced by TFMGs, outlook, and proposed solutions.

TFMGs as overcoats open a wide window for biomedical engineers to be explored. There are challenges allied with the development of TFMGs in the biomedical application, for e.g., the development of TFMGs without the inclusion of toxic elements (Ni, Be), but with good GFA is a challenge in the biosafety concerns. The TFMG with good GFA that comprises a noble metal, namely palladium (Pd), increases production costs. These issues may seriously impede the wide-reaching applications of TFMGs in bioimplants applications. Thus, eliminating the noble elements and the toxic elements with greater GFA in TFMGs will be another challenge and research direction in the development of TFMGs for biomedical applications. Combinatorial magnetron co-sputtering techniques can be employed to design and fabricate TFMGs composition library with different physical, chemical and biological properties.

TFMG with antibacterial activity and biocompatibility or non-toxicity is another challenge. Ag and Cu are good substitutions to inhibit bacterial colonies and adhesion. But when their concentration is higher, they induce toxicity to tissues or human cells, so their percentage used in the alloy should be antibacterial as well as non-toxic to human cells. Additionally, surface modification, such as the formation of nanopillars or nanostructures produced by ion etching, inhibits bacterial growth and enhances the growth of tissues or human cells [134]. These nanostructures fabricated should be capable of segregating bacteria and enhance tissue cells and cellular function. Therefore, the future trend will combine biocompatible and antibacterial coating material or the nanostructured surface to promote human cell growth and resist bacterial adhesion. This approach can be used in a wide range of biomedical applications.

Multi-functional or multilayered coatings have been developed to attain their desired properties of biomaterials surface. The biomaterial's biological and mechanical properties are selectively improved by modifying the TFMG surfaces by overcoats while the features of the TFMGs are retained. The multilayered coatings will certainly magnify its use in the biomedical field. The bone biomaterial interface binding can be attained by combining different coatings (e.g. HaP or Bio glasses) with different techniques. Additionally, the creation of mesh-like or porous structured overcoats promote bone growth at the interface and upsurge implant fixation and heals earlier [135]. Considering this fact, multifunctional or multilayered coatings on TFMGs for biomedical applications is one of the essential directions for further studies.

9. Conclusions

Research over a couple of decades has developed a large number of TFMGs of different composition, inspiring intense research consideration in the search for novel physical and chemical phenomena in non-equilibrium, disordered, multicomponent films. TFMGs provide great promise as one of the best coatings for surface modification of biomedical materials and devices. In the present review,

an effort is made to cover the mechanical and thermal properties, corrosion, and biological response of specific TFMGs based on Zr, Ti, Fe and Mg. It is noteworthy that the biodegradable Mg-based metallic glasses progressively degrade in the human environment after serving their purpose. Degradable metallic glasses (both bulk and thin films) are sparingly reported and open a new area to be explored further. These remarkable properties of TFMGs lead them directly to beneficial biomedical applications such as bioimplants and surgical devices.

Declaration of Competing Interest

The authors declare that they have no known competing financial interests or personal relationships that could have appeared to influence the work reported in this paper.

Acknowledgements

The authors hereby acknowledge the funding obtained Indian Institute of Technology Madras, India (IIT Madras) (SB20210850MMMHRD008275) through Institute of Eminence. One of the authors S Thanka Rajan thank the IIT Madras, Chennai for providing him the post-doctoral fellowship (IPDF) and the research grant for this research.

References

[1] A.B. Hazar Yoru, B. Cem, Biomaterials, in: A.B. H.Y., B.C. Şener (Eds.), A Roadmap Biomed. Eng. Milestones, InTech, 2012, pp. 55–58, https://doi.org/10.5772/48057
[2] J. Davis (Ed.), Handbook of Materials for Medical Devices, first ed., ASM International, Ohio, 2003, , https://doi.org/10.1361/hmmd2003p001
[3] C.W. Kang, F.Z. Fang, State of the art of bioimplants manufacturing: part I, Adv. Manuf. 6 (2018) 20–40, https://doi.org/10.1007/s40436-017-0207-4
[4] K. Prasad, O. Bazaka, M. Chua, M. Rochford, L. Fedrick, J. Spoor, R. Symes, M. Tieppo, C. Collins, A. Cao, D. Markwell, K. (Ken) Ostrikov, K. Bazaka, Metallic biomaterials: current challenges and opportunities, Materials 10 (2017) 884, https://doi.org/10.3390/ma10080884
[5] K.E. Tanner, Titanium in Medicine, (2002), ⟨https://doi.org/10.1243/0954411021536432⟩.
[6] P.I. Brånemark, B.O. Hansson, R. Adell, U. Breine, J. Lindström, O. Hallén, A. Ohman, Osseointegrated implants in the treatment of the edentulous jaw. Experience from a 10-year period. Scand. J. Plast. Reconstr. Surg. Suppl. 16 (1977) 1–132 ⟨http://www.ncbi.nlm.nih.gov/pubmed/356184⟩.
[7] T. Hanawa, Titanium–tissue interface reaction and its control with surface treatment, Front. Bioeng. Biotechnol. 7 (2019) 1–13, https://doi.org/10.3389/fbioe.2019.00170
[8] T. Hanawa, An overview of biofunctionalization of metals in Japan, J. R. Soc. Interface 6 (2009) S361–S369, https://doi.org/10.1098/rsif.2008.0427.focus
[9] E.J. Kelly, Electrochemical behavior of titanium, in: W.R. Bockris J.O., B.E. Conway (Eds.), Modern Aspects of Electrochemistry, Springer, US, Boston, MA, 1982, pp. 319–424, https://doi.org/10.1007/978-1-4615-7458-3_5
[10] S. Thanka Rajan, A. Bendavid, B. Subramanian, Cytocompatibility assessment of Ti-Nb-Zr-Si thin film metallic glasses with enhanced osteoblast differentiation for biomedical applications, Colloids Surf. B Biointerfaces 173 (2019) 109–120, https://doi.org/10.1016/j.colsurfb.2018.09.041
[11] B. Basu, D.S. Katti, A. Kumar, Advanced Biomaterials: Fundamentals, Processing, and Applications, (2009).
[12] S. Thanka Rajan, M. Karthika, A. Bendavid, B. Subramanian, Apatite layer growth on glassy $Zr_{48}Cu_{36}Al_8Ag_8$ sputtered titanium for potential biomedical applications, Appl. Surf. Sci. 369 (2016) 501–509, https://doi.org/10.1016/j.apsusc.2016.02.054
[13] A.R. Yavari, A new order for metallic glasses, Nature 439 (2006) 405–406, https://doi.org/10.1038/439405a
[14] M. Chen, A brief overview of bulk metallic glasses, NPG Asia Mater. 3 (2011) 82–90, https://doi.org/10.1038/asiamat.2011.30
[15] P. Meagher, E.D. O'Cearbhaill, J.H. Byrne, D.J. Browne, Bulk metallic glasses for implantable medical devices and surgical tools, Adv. Mater. 28 (2016) 5755–5762, https://doi.org/10.1002/adma.201505347
[16] J.J. Kruzic, Bulk metallic glasses as structural materials: a review, Adv. Eng. Mater. 18 (2016) 1308–1331, https://doi.org/10.1002/adem.201600066
[17] A. Inoue, B. Shen, N. Nishiyama, Development and applications of late transition metal bulk metallic glasses, Bulk Met. Glass. 18 (2008) 1–25, https://doi.org/10.1007/978-0-387-48921-6_1
[18] M.D. Demetriou, A. Wiest, D.C. Hofmann, W.L. Johnson, B. Han, N. Wolfson, G. Wang, P.K. Liaw, Amorphous metals for hard-tissue prosthesis, JOM 62 (2010) 83–91, https://doi.org/10.1007/s11837-010-0038-2
[19] H.F. Li, Y.F. Zheng, Recent advances in bulk metallic glasses for biomedical applications, Acta Biomater. 36 (2016) 1–20, https://doi.org/10.1016/j.actbio.2016.03.047
[20] W. Klement, R.H. Willens, P. Duwez, Non-crystalline structure in solidified gold–silicon alloys, Nature 187 (1960) 869–870, https://doi.org/10.1038/187869b0
[21] H. Chen, Thermodynamic considerations on the formation and stability of metallic glasses, Acta Met. 22 (1974) 1505–1511, https://doi.org/10.1016/0001-6160(74)90112-6
[22] P. Gong, L. Deng, J. Jin, S. Wang, X. Wang, K. Yao, Review on the research and development of ti-based bulk metallic glasses, Metals 6 (2016) 264, https://doi.org/10.3390/met6110264
[23] P. Meagher, E.D.O. Cearbhaill, J.H. Byrne, D.J. Browne, Bulk metallic glasses for implantable medical devices and surgical tools, Adv. Mater. 28 (2016) 5755–5762, https://doi.org/10.1002/adma.201505347
[24] X. Gu, Y. Zheng, S. Zhong, T. Xi, J. Wang, W. Wang, Corrosion of, and cellular responses to Mg-Zn-Ca bulk metallic glasses, Biomaterials 31 (2010) 1093–1103, https://doi.org/10.1016/j.biomaterials.2009.11.015
[25] G. Han, J.-Y. Lee, Y.-C. Kim, J.H. Park, D.-I. Kim, H.-S. Han, S.-J. Yang, H.-K. Seok, Preferred crystallographic pitting corrosion of pure magnesium in Hanks' solution, Corros. Sci. 63 (2012) 316–322, https://doi.org/10.1016/j.corsci.2012.06.011
[26] S.T. Rajan, A.K. Nanda Kumar, B. Subramanian, Nanocrystallization in magnetron sputtered Zr–Cu–Al–Ag thin film metallic glasses, CrystEngComm 16 (2014) 2835–2844, https://doi.org/10.1039/c3ce42294a
[27] X.H. Lin, W.L. Johnson, Formation of Ti–Zr–Cu–Ni bulk metallic glasses, J. Appl. Phys. 78 (1995) 6514–6519, https://doi.org/10.1063/1.360537
[28] C.H. Huang, J.C. Huang, J.B. Li, J.S.C. Jang, Simulated body fluid electrochemical response of Zr-based metallic glasses with different degrees of crystallization, Mater. Sci. Eng. C 33 (2013) 4183–4187, https://doi.org/10.1016/j.msec.2013.06.007
[29] C.J. Chen, J.C. Huang, H.S. Chou, Y.H. Lai, L.W. Chang, X.H. Du, J.P. Chu, T.G. Nieh, On the amorphous and nanocrystalline Zr–Cu and Zr–Ti co-sputtered thin films, J. Alloy. Compd. 483 (2009) 337–340, https://doi.org/10.1016/j.jallcom.2008.07.188
[30] H.S. Chou, J.C. Huang, L.W. Chang, Mechanical properties of ZrCuTi thin film metallic glass with high content of immiscible tantalum, Surf. Coat. Technol. 205 (2010) 587–590, https://doi.org/10.1016/j.surfcoat.2010.07.042
[31] B. Subramanian, S. Maruthamuthu, S.T. Rajan, Biocompatibility evaluation of sputtered zirconium-based thin film metallic glass-coated steels, Int. J. Nanomed. 10 (2015) 17–29, https://doi.org/10.2147/IJN.S79977
[32] G.A. Almyras, G.M. Matenoglou, P. Komninou, C. Kosmidis, P. Patsalas, G.A. Evangelakis, On the deposition mechanisms and the formation of glassy Cu–Zr thin films, J. Appl. Phys. 107 (2010) 084313, https://doi.org/10.1063/1.3366715
[33] J.P. Chu, J.S.C. Jang, J.C. Huang, H.S. Chou, Y. Yang, J.C. Ye, Y.C. Wang, J.W. Lee, F.X. Liu, P.K. Liaw, Y.C. Chen, C.M. Lee, C.L. Li, C. Rullyani, Thin film metallic glasses: unique properties and potential applications, Thin Solid Films 520 (2012) 5097–5122, https://doi.org/10.1016/j.tsf.2012.03.092
[34] S. Das, R. Santos-Ortiz, H.S. Arora, S. Mridha, N.D. Shepherd, S. Mukherjee, Electromechanical behavior of pulsed laser deposited platinum-based metallic glass thin films, Phys. Status Solidi Appl. Mater. Sci. 213 (2016) 399–404, https://doi.org/10.1002/pssa.201532639
[35] I. James J. Myrick, Glencoe, Amorphous Metal Deposition And New Aluminum-based Amorphous Metals, US 2005/0123686A1, 2005, ⟨https://patents.google.com/patent/US20050123686A1/en⟩.
[36] J.P. Chu, J.C. Huang, J.S.C. Jang, Y.C. Wang, P.K. Liaw, Thin film metallic glasses: preparations, properties, and applications, JOM 62 (2010) 19–24, https://doi.org/10.1007/s11837-010-0053-3
[37] P. Yiu, W. Diyatmika, N. Bönninghoff, Y.C. Lu, B.Z. Lai, J.P. Chu, Thin film metallic glasses: properties, applications and future, J. Appl. Phys. 127 (2020) 030901, https://doi.org/10.1063/1.5122884
[38] S. Korkmaz, A. Kariper, Glass formation, production and superior properties of Zr-based thin film metallic glasses (TFMGs): a status review, J. Non-Cryst. Solids 527 (2020) 119753, https://doi.org/10.1016/j.jnoncrysol.2019.119753
[39] M. Apreutesei, P. Steyer, A. Billard, L. Joly-Pottuz, C. Esnouf, Zr-Cu thin film metallic glasses: an assessment of the thermal stability and phases' transformation mechanisms, J. Alloy. Compd. 619 (2015) 284–292, https://doi.org/10.1016/j.jallcom.2014.08.253
[40] K.-W. Park, J. Jang, M. Wakeda, Y. Shibutani, J.-C. Lee, Atomic packing density and its influence on the properties of Cu–Zr amorphous alloys, Scr. Mater. 57 (2007) 805–808, https://doi.org/10.1016/j.scriptamat.2007.07.019
[41] A. Rauf, C.Y. Guo, Y.N. Fang, Z. Yu, B.A. Sun, T. Feng, Binary Cu-Zr thin film metallic glasses with tunable nanoscale structures and properties, J. Non Cryst. Solids 498 (2018) 95–102, https://doi.org/10.1016/j.jnoncrysol.2018.06.015
[42] C.Y. Chuang, J.W. Lee, C.L. Li, J.P. Chu, Mechanical properties study of a magnetron-sputtered Zr-based thin film metallic glass, Surf. Coat. Technol. 215 (2013) 312–321, https://doi.org/10.1016/j.surfcoat.2012.04.101
[43] J.C. Ye, J.P. Chu, Y.C. Chen, Q. Wang, Y. Yang, Hardness, yield strength, and plastic flow in thin film metallic-glass, J. Appl. Phys. 112 (2012) 053516, https://doi.org/10.1063/1.4750028
[44] P.S. Chen, H.W. Chen, J.G. Duh, J.W. Lee, J. Shian-Ching Jang, Mechanical and thermal behaviors of nitrogen-doped Zr-Cu-Al-Ag-Ta-–An alternative class of thin film metallic glass, Appl. Phys. Lett. 101 (2012) 181902, https://doi.org/10.1063/1.4759035

[45] G.I. Nkou Bouala, A. Etiemble, C. Der Loughian, C. Langlois, J.-F. Pierson, P. Steyer, Silver influence on the antibacterial activity of multi-functional Zr-Cu based thin film metallic glasses, Surf. Coat. Technol. 343 (2018) 108–114, https://doi.org/10.1016/j.surfcoat.2017.10.057

[46] A. Jabed, M.M. Khan, J. Camiller, M. Greenlee-Wacker, W. Haider, I. Shabib, Property optimization of Zr-Ti-X (X = Ag, Al) metallic glass via combinatorial development aimed at prospective biomedical application, Surf. Coat. Technol. 372 (2019) 278–287, https://doi.org/10.1016/j.surfcoat.2019.05.036

[47] C.N. Cai, C. Zhang, Y.S. Sun, H.H. Huang, C. Yang, L. Liu, ZrCuFeAlAg thin film metallic glass for potential dental applications, Intermetallics 86 (2017) 80–87, https://doi.org/10.1016/j.intermet.2017.03.016

[48] S. Korkmaz, İ. Af, Glass formation, production and superior properties of Zr-based thin fi lm metallic glasses (TFMGs): a status review, J. Non-Cryst. Solids 527 (2020) 119753, https://doi.org/10.1016/j.jnoncrysol.2019.119753

[49] M. Apreutesei, P. Steyer, L. Joly-Pottuz, A. Billard, J. Qiao, S. Cardinal, F. Sanchette, J.M. Pelletier, C. Esnouf, Microstructural, thermal and mechanical behavior of co-sputtered binary Zr-Cu thin film metallic glasses, Thin Solid Films 561 (2014) 53–59, https://doi.org/10.1016/j.tsf.2013.05.177

[50] J.H. Chu, H.W. Chen, Y.C. Chan, J.G. Duh, J.W. Lee, J.S.C. Jang, Modification of structure and property in Zr-based thin film metallic glass via processing temperature control, Thin Solid Films 561 (2014) 38–42, https://doi.org/10.1016/j.tsf.2013.05.179

[51] T.P. Hsiao, Y.C. Yang, J.W. Lee, C.L. Li, J.P. Chu, The microstructure and mechanical properties of nitrogen and boron contained ZrCuAlNi thin film metallic glass composites, Surf. Coat. Technol. 237 (2013) 276–283, https://doi.org/10.1016/j.surfcoat.2013.09.015

[52] S. Thanka Rajan, M. Karthika, A. Bendavid, B. Subramanian, Apatite layer growth on glassy $Zr_{48}Cu_{36}Al_8Ag_8$ sputtered titanium for potential biomedical applications, Appl. Surf. Sci. 369 (2016) 501–509, https://doi.org/10.1016/j.apsusc.2016.02.054

[53] X.P. Nie, X.H. Yang, L.Y. Chen, K.B. Yeap, K.Y. Zeng, D. Li, J.S. Pan, X.D. Wang, Q.P. Cao, S.Q. Ding, J.Z. Jiang, The effect of oxidation on the corrosion resistance and mechanical properties of a Zr-based metallic glass, Corros. Sci. 53 (2011) 3557–3565, https://doi.org/10.1016/j.corsci.2011.06.032

[54] C.H. Lin, C.H. Huang, J.F. Chuang, H.C. Lee, M.C. Liu, X.H. Du, J.C. Huang, J.S.C. Jang, C.H. Chen, Simulated body-fluid tests and electrochemical investigations on biocompatibility of metallic glasses, Mater. Sci. Eng. C 32 (2012) 2578–2582, https://doi.org/10.1016/j.msec.2012.07.043

[55] N. Hua, L. Huang, W. Chen, W. He, T. Zhang, Biocompatible Ni-free Zr-based bulk metallic glasses with high-Zr-content: Compositional optimization for potential biomedical applications, Mater. Sci. Eng. C 44 (2014) 400–410, https://doi.org/10.1016/j.msec.2014.08.049

[56] Y. Sun, Y. Huang, H. Fan, F. Liu, J. Shen, J. Sun, J.J.J. Chen, Comparison of mechanical behaviors of several bulk metallic glasses for biomedical application, J. Non Cryst. Solids 406 (2014) 144–150, https://doi.org/10.1016/j.jnoncrysol.2014.09.021

[57] L. Huang, C. Pu, R.K. Fisher, D.J.H. Mountain, Y. Gao, P.K. Liaw, W. Zhang, W. He, A Zr-based bulk metallic glass for future stent applications: materials properties, finite element modeling, and in vitro human vascular cell response, Acta Biomater. 25 (2015) 356–368, https://doi.org/10.1016/j.actbio.2015.07.012

[58] F.X. Liu, F.Q. Yang, Y.F. Gao, W.H. Jiang, Y.F. Guan, P.D. Rack, O. Sergic, P.K. Liaw, Micro-scratch study of a magnetron-sputtered Zr-based metallic-glass film, Surf. Coat. Technol. 203 (2009) 3480–3484, https://doi.org/10.1016/j.surfcoat.2009.05.017

[59] P.H. Tsai, Y.Z. Lin, J.B. Li, S.R. Jian, J.S.C. Jang, C. Li, J.P. Chu, J.C. Huang, Sharpness improvement of surgical blade by means of ZrCuAlAgSi metallic glass and metallic glass thin film coating, Intermetallics 31 (2012) 127–131, https://doi.org/10.1016/j.intermet.2012.06.014

[60] P.H. Tsai, T.H. Li, K.T. Hsu, J.W. Chiou, J.S.C. Jang, J.P. Chu, Effect of coating thickness on the cutting sharpness and durability of Zr-based metallic glass thin film coated surgical blades, Thin Solid Films 618 (2016) 36–41, https://doi.org/10.1016/j.tsf.2016.05.020

[61] J.P. Chu, C.C. Yu, Y. Tanatsugu, M. Yasuzawa, Y.L. Shen, Non-stick syringe needles: Beneficial effects of thin film metallic glass coating, Sci. Rep. 6 (2016) 31847, https://doi.org/10.1038/srep31847

[62] M.Y. Bai, Y.C. Chang, J.P. Chu, Preclinical studies of non-stick thin film metallic glass-coated syringe needles, Sci. Rep. 10 (2020) 1–11, https://doi.org/10.1038/s41598-020-77008-y

[63] S.T. Rajan, A.T.V. V, M. Terada-Nakaishi, P. Chen, T. Hanawa, A.K. Nandakumar, B. Subramanian, Zirconium-based metallic glass and zirconia coatings to inhibit bone formation on titanium, Biomed. Mater. 15 (2020) 065019, https://doi.org/10.1088/1748-605X/aba23a

[64] J.L. Ke, C.H. Huang, Y.H. Chen, W.Y. Tsai, T.Y. Wei, J.C. Huang, In vitro biocompatibility response of Ti-Zr-Si thin film metallic glasses, Appl. Surf. Sci. 322 (2014) 41–46, https://doi.org/10.1016/j.apsusc.2014.09.204

[65] J.C. Chang, J.W. Lee, B.S. Lou, C.L. Li, J.P. Chu, Effects of tungsten contents on the microstructure, mechanical and anticorrosion properties of Zr-W-Ti thin film metallic glasses, Thin Solid Films 584 (2015) 253–256, https://doi.org/10.1016/j.tsf.2015.01.063

[66] L. Liu, C.L. Qiu, Q. Chen, K.C. Chan, S.M. Zhang, Deformation behavior, corrosion resistance, and cytotoxicity of Ni-free Zr-based bulk metallic glasses, J. Biomed. Mater. Res. Part A 86A (2008) 160–169, https://doi.org/10.1002/jbm.a.31425

[67] C.Y. Chuang, Y.C. Liao, J.W. Lee, C.L. Li, J.P. Chu, J.G. Duh, Electrochemical characterization of Zr-based thin film metallic glass in hydrochloric aqueous solution, Thin Solid Films 529 (2013) 338–341, https://doi.org/10.1016/j.tsf.2012.03.065

[68] N. Hua, L. Huang, J. Wang, Y. Cao, W. He, S. Pang, T. Zhang, Corrosion behavior and in vitro biocompatibility of Zr–Al–Co–Ag bulk metallic glasses: an experimental case study, J. Non Cryst. Solids 358 (2012) 1599–1604, https://doi.org/10.1016/j.jnoncrysol.2012.04.022

[69] L. Liu, C.L. Qiu, Q. Chen, S.M. Zhang, Corrosion behavior of Zr-based bulk metallic glasses in different artificial body fluids, J. Alloy. Compd. 425 (2006) 268–273, https://doi.org/10.1016/j.jallcom.2006.01.048

[70] A. Kawashima, K. Ohmura, Y. Yokoyama, A. Inoue, The corrosion behaviour of Zr-based bulk metallic glasses in 0.5M NaCl solution, Corros. Sci. 53 (2011) 2778–2784, https://doi.org/10.1016/j.corsci.2011.05.014

[71] X.P. Nie, Q.P. Cao, Z.F. Wu, Y. Ma, X.D. Wang, S.Q. Ding, J.Z. Jiang, The pitting corrosion behavior of shear bands in a Zr-based bulk metallic glass, Scr. Mater. 67 (2012) 376–379, https://doi.org/10.1016/j.scriptamat.2012.05.025

[72] Y. Zhang, L. Yan, X. Zhao, L. Ma, Enhanced chloride ion corrosion resistance of Zr-based bulk metallic glasses with cobalt substitution, J. Non Cryst. Solids 496 (2018) 18–23, https://doi.org/10.1016/j.jnoncrysol.2018.05.005

[73] J. Tang, Q. Zhu, Y. Wang, M. Apreutesei, H. Wang, P. Steyer, M. Chamas, A. Billard, Insights on the role of copper addition in the corrosion and mechanical properties of binary Zr-Cu metallic glass coatings, Coatings 7 (2017) 223, https://doi.org/10.3390/coatings7120223

[74] A. Gebert, P.F. Gostin, L. Schultz, Effect of surface finishing of a Zr-based bulk metallic glass on its corrosion behaviour, Corros. Sci. 52 (2010) 1711–1720, https://doi.org/10.1016/j.corsci.2010.01.027

[75] J. Jayaraj, A. Gebert, L. Schultz, Passivation behaviour of structurally relaxed Zr48Cu36Ag8Al8 metallic glass, J. Alloy. Compd. 479 (2009) 257–261, https://doi.org/10.1016/j.jallcom.2009.01.056

[76] N. Homazava, A. Shkabko, D. Logvinovich, U. Krähenbühl, A. Ulrich, Element-specific in situ corrosion behavior of Zr–Cu–Ni–Al–Nb bulk metallic glass in acidic media studied using a novel microcapillary flow injection inductively coupled plasma mass spectrometry technique, Intermetallics 16 (2008) 1066–1072, https://doi.org/10.1016/j.intermet.2008.06.005

[77] J.P. Chu, T.-Y. Liu, C.-L. Li, C.-H. Wang, J.S.C. Jang, M.-J. Chen, S.-H. Chang, W.-C. Huang, Fabrication and characterizations of thin film metallic glasses: antibacterial property and durability study for medical application, Thin Solid Films 561 (2014) 102–107, https://doi.org/10.1016/j.tsf.2013.08.111

[78] A. Etiemble, C. Der Loughian, M. Apreutesei, C. Langlois, S. Cardinal, J.M. Pelletier, J.F. Pierson, P. Steyer, Innovative Zr-Cu-Ag thin film metallic glass deposed by magnetron PVD sputtering for antibacterial applications, J. Alloy. Compd. 707 (2017) 155–161, https://doi.org/10.1016/j.jallcom.2016.12.259

[79] Y. Liu, J. Padmanabhan, B. Cheung, J. Liu, Z. Chen, B.E. Scanley, D. Wesolowski, M. Pressley, C.C. Broadbridge, S. Altman, U.D. Schwarz, T.R. Kyriakides, J. Schroers, Combinatorial development of antibacterial Zr-Cu-Al-Ag thin film metallic glasses, Sci. Rep. 6 (2016) 1–8, https://doi.org/10.1038/srep26950

[80] W. Diyatmika, C.C. Yu, Y. Tanatsugu, M. Yasuzawa, J.P. Chu, Fibrinogen and albumin adsorption profiles on Ni-free Zr-based thin film metallic glass, Thin Solid Films 688 (2019) 137382, https://doi.org/10.1016/j.tsf.2019.06.032

[81] N. Hua, L. Huang, W. Chen, W. He, T. Zhang, Biocompatible Ni-free Zr-based bulk metallic glasses with high-Zr-content: compositional optimization for potential biomedical applications, Mater. Sci. Eng. C 44 (2014) 400–410, https://doi.org/10.1016/j.msec.2014.08.049

[82] A. Jabed, Z.U. Rahman, M.M. Khan, W. Haider, I. Shabib, Combinatorial development and in vitro characterization of the quaternary Zr–Ti–X–Y (X–Y = Cu–Ag/Co–Ni) metallic glass for prospective bioimplants, Adv. Eng. Mater. 21 (2019) 1–12, https://doi.org/10.1002/adem.201900726

[83] A. Blanquer, A. Hynowska, C. Nogués, E. Ibáñez, J. Sort, M.D. Baró, B. Özkale, S. Pané, E. Pellicer, L. Barrios, Effect of surface modifications of $Ti_{40}Zr_{10}Cu_{38}Pd_{12}$ bulk metallic glass and Ti-6Al-4V alloy on human osteoblasts in vitro biocompatibility, PLoS One 11 (2016) 1–15, https://doi.org/10.1371/journal.pone.0156644

[84] S. Thanka Rajan, A.K. Nandakumar, T. Hanawa, B. Subramanian, Materials properties of ion beam sputtered Ti-Cu-Pd-Zr thin film metallic glasses, J. Non Cryst. Solids 461 (2017) 104–112, https://doi.org/10.1016/j.jnoncrysol.2017.01.008

[85] J. Kobata, K. Miura, K. Amiya, Y. Fukuda, Y. Saotome, Nanoimprinting of Ti–Cu-based thin-film metallic glasses deposited by unbalanced magnetron sputtering, J. Alloy. Compd. 707 (2017) 132–136, https://doi.org/10.1016/j.jallcom.2016.11.174

[86] J. Kobata, K. Miura, Effects of Ar ion bombardment by unbalanced magnetron sputtering on mechanical and thermal properties of Ti-Cu-Zr-Ni-Hf-Si thin film metallic glass, Mater. Des. 111 (2016) 271–278, https://doi.org/10.1016/j.matdes.2016.09.005

[87] J. Sakurai, S. Hata, Search for Ti–Ni–Zr thin film metallic glasses exhibiting a shape memory effect after crystallization, Mater. Sci. Eng. A 541 (2012) 8–13, https://doi.org/10.1016/j.msea.2012.01.075

[88] C.H. Lin, C.H. Huang, J.F. Chuang, J.C. Huang, J.S.C. Jang, C.H. Chen, Rapid screening of potential metallic glasses for biomedical applications, Mater. Sci. Eng. C 33 (2013) 4520–4526, https://doi.org/10.1016/j.msec.2013.07.006

[89] M. Sarafbidabad, Synthesis of Ti-based metallic glass thin film in high vacuum pressure on 316 L stainless steel, Thin Solid Films 574 (2015) 189–195, https://doi.org/10.1016/j.tsf.2014.11.080

[90] T.H. Li, P.C. Wong, S.F. Chang, P.H. Tsai, J.S.C. Jang, J.C. Huang, Biocompatibility study on Ni-free Ti-based and Zr-based bulk metallic glasses, Mater. Sci. Eng. C 75 (2017) 1–6, https://doi.org/10.1016/j.msec.2017.02.006

[91] B. Subramanian, In vitro corrosion and biocompatibility screening of sputtered Ti40Cu36Pd14Zr10 thin film metallic glasses on steels, Mater. Sci. Eng. C 47 (2015) 48–56, https://doi.org/10.1016/j.msec.2014.11.013

[92] S. Thanka Rajan, A.K. Nandakumar, T. Hanawa, B. Subramanian, Materials properties of ion beam sputtered Ti-Cu-Pd-Zr thin film metallic glasses, J. Non-Cryst. Solids 461 (2017) 104–112, https://doi.org/10.1016/j.jnoncrysol.2017.01.008
[93] S.L. Zhu, X.M. Wang, F.X. Qin, A. Inoue, A new Ti-based bulk glassy alloy with potential for biomedical application, Mater. Sci. Eng. A 459 (2007) 233–237, https://doi.org/10.1016/j.msea.2007.01.044
[94] J.-J. Oak, D.V. Louzguine-Luzgin, A. Inoue, Fabrication of Ni-free Ti-based bulk-metallic glassy alloy having potential for application as biomaterial, and investigation of its mechanical properties, corrosion, and crystallization behavior, J. Mater. Res. 22 (2007) 1346–1353, https://doi.org/10.1557/jmr.2007.0154
[95] J.-J. Oak, D.V. Louzguine-Luzgin, A. Inoue, Investigation of glass-forming ability, deformation and corrosion behavior of Ni-free Ti-based BMG alloys designed for application as dental implants, Mater. Sci. Eng. C 29 (2009) 322–327, https://doi.org/10.1016/j.msec.2008.07.009
[96] Q. Zhou, Y. Du, Q. Jia, W. Han, X. Zhao, Y. Deng, H. Wang, A nanoindentation study of Ti-based high entropy bulk metallic glasses at elevated temperatures, J. Non-Cryst. Solids 532 (2020) 119878, https://doi.org/10.1016/j.jnoncrysol.2019.119878
[97] L. Huang, X. Hu, T. Guo, S. Li, Investigation of mechanical properties and plastic deformation behavior of (Tiurilmetallic) glasses by nanoindentation, Adv. Mater. Sci. Eng. 2014 (2014) 2–7, https://doi.org/10.1155/2014/215093
[98] Y.B. Wang, H.F. Li, Y. Cheng, Y.F. Zheng, L.Q. Ruan, In vitro and in vivo studies on Ti-based bulk metallic glass as potential dental implant material, Mater. Sci. Eng. C 33 (2013) 3489–3497, https://doi.org/10.1016/j.msec.2013.04.038
[99] S. Pang, Y. Liu, H. Li, L. Sun, Y. Li, T. Zhang, New Ti-based Ti–Cu–Zr–Fe–Sn–Si–Ag bulk metallic glass for biomedical applications, J. Alloy. Compd. 625 (2015) 323–327, https://doi.org/10.1016/j.jallcom.2014.07.021
[100] C.H. Huang, Y.S. Huang, Y.S. Lin, C.H. Lin, J.C. Huang, C.H. Chen, J.B. Li, Y.H. Chen, J.S.C. Jang, Electrochemical and biocompatibility response of newly developed TiZr-based metallic glasses, Mater. Sci. Eng. C 43 (2014) 343–349, https://doi.org/10.1016/j.msec.2014.06.040
[101] J.J. Oak, D.V. Louzguine-Luzgin, A. Inoue, Investigation of glass-forming ability, deformation and corrosion behavior of Ni-free Ti-based BMG alloys designed for application as dental implants, Mater. Sci. Eng. C 29 (2009) 322–327, https://doi.org/10.1016/j.msec.2008.07.009
[102] S.P. Wang, J. Xu, TiZrNbTaMo high-entropy alloy designed for orthopedic implants: as-cast microstructure and mechanical properties, Mater. Sci. Eng. C 73 (2017) 80–89, https://doi.org/10.1016/j.msec.2016.12.057
[103] S. Abdi, S. Oswald, P.F. Gostin, A. Helth, J. Sort, M.D. Barõ, M. Calin, L. Schultz, J. Eckert, A. Gebert, Designing new biocompatible glass-forming Ti75-xZr10NbxSi15 (x = 0, 15) alloys: corrosion, passivity, and apatite formation, J. Biomed. Mater. Res. Part B Appl. Biomater. 104 (2016) 27–38, https://doi.org/10.1002/jbm.b.33332
[104] S. Tantavisut, B. Lohwongwatana, A. Khamkongkaeo, A. Tanavalee, P. Tangpornprasert, P. Ittiravivong, The novel toxic free titanium-based amorphous alloy for biomedical application, J. Mater. Res. Technol. 7 (2018) 248–253, https://doi.org/10.1016/j.jmrt.2017.08.007
[105] B.S. Lou, Y.C. Yang, J.W. Lee, L.T. Chen, Biocompatibility and mechanical property evaluation of Zr-Ti-Fe based ternary thin film metallic glasses, Surf. Coat. Technol. 320 (2017) 512–519, https://doi.org/10.1016/j.surfcoat.2016.11.039
[106] J.S.C. Jang, P.H. Tsai, A.Z. Shiao, T.H. Li, C.Y. Chen, J.P. Chu, J.G. Duh, M.J. Chen, S.-H. Chang, W.-C. Huang, Enhanced cutting durability of surgical blade by coating with Fe-based metallic glass thin film, Intermetallics 65 (2015) 56–60, https://doi.org/10.1016/j.intermet.2015.06.012
[107] A. Inoue, Stabilization of metallic supercooled liquid and bulk amorphous alloys, Acta Mater. 48 (2000) 279–306, https://doi.org/10.1016/S1359-6454(99)00300-6
[108] L.T. Chen, J.W. Lee, Y.C. Yang, B.S. Lou, C.L. Li, J.P. Chu, Microstructure, mechanical and anti-corrosion property evaluation of iron-based thin film metallic glasses, Surf. Coat. Technol. 260 (2014) 46–55, https://doi.org/10.1016/j.surfcoat.2014.07.039
[109] H.S. Ni, X.H. Liu, X.C. Chang, W.L. Hou, W. Liu, J.Q. Wang, High performance amorphous steel coating prepared by HVOF thermal spraying, J. Alloy. Compd. 467 (2009) 163–167, https://doi.org/10.1016/j.jallcom.2007.11.133
[110] T.A. Phan, S.M. Lee, A. Makino, H. Oguchi, H. Kuwano, FE-B-NB-ND magnetic metallic glass thin film for MEMS/NEMS structure, in: Proceedings of the IEEE International Conference on Micro Electro Mechanical Systems, 2011, pp. 428–431, doi: ⟨10.1109/MEMSYS.2011.5734453⟩.
[111] T.A. Phan, H. Oguchi, M. Hara, M. Shikida, H. Hida, T. Ando, K. Sato, H. Kuwano, Fe-B-Nd-Nb metallic glass thin films for microelectromechanical systems, Appl. Phys. Lett. 103 (2013) 10–14, https://doi.org/10.1063/1.4826443
[112] B.S. Lou, T.Y. Lin, W.T. Chen, J.W. Lee, Corrosion property and biocompatibility evaluation of Fe–Zr–Nb thin film metallic glasses, Thin Solid Films 691 (2019) 137615, https://doi.org/10.1016/j.tsf.2019.137615
[113] A. Obeydavi, A. Shafyei, A. Rezaeian, P. Kameli, J.W. Lee, Microstructure, mechanical properties and corrosion performance of $Fe_{44}Cr_{15}Mo_{14}Co_7C_{10}B_5Si_5$ thin film metallic glass deposited by DC magnetron sputtering, J. Non-Cryst. Solids 527 (2020) 119718, https://doi.org/10.1016/j.jnoncrysol.2019.119718
[114] X.J. Gu, S.J. Poon, G.J. Shiflet, Mechanical properties of iron-based bulk metallic glasses, J. Mater. Res. 22 (2007) 344–351, https://doi.org/10.1557/jmr.2007.0036
[115] X.J. Gu, S.J. Poon, G.J. Shiflet, Effects of carbon content on the mechanical properties of amorphous steel alloys, Scr. Mater. 57 (2007) 289–292, https://doi.org/10.1016/j.scriptamat.2007.05.006
[116] X.J. Gu, S.J. Poon, G.J. Shiflet, M. Widom, Ductility improvement of amorphous steels: roles of shear modulus and electronic structure, Acta Mater. 56 (2008) 88–94, https://doi.org/10.1016/j.actamat.2007.09.011
[117] B.S. Lou, T.Y. Lin, W.T. Chen, J.W. Lee, Corrosion property and biocompatibility evaluation of Fe–Zr–Nb thin film metallic glasses, Thin Solid Films 691 (2019) 137615, https://doi.org/10.1016/j.tsf.2019.137615
[118] Z. Li, C. Zhang, L. Liu, Wear behavior and corrosion properties of Fe-based thin film metallic glasses, J. Alloy. Compd. 650 (2015) 127–135, https://doi.org/10.1016/j.jallcom.2015.07.256
[119] Y.B. Wang, H.F. Li, Y.F. Zheng, M. Li, Corrosion performances in simulated body fluids and cytotoxicity evaluation of Fe-based bulk metallic glasses, Mater. Sci. Eng. C 32 (2012) 599–606, https://doi.org/10.1016/j.msec.2011.12.018
[120] N. Padhy, S. Ningshen, U. Kamachi Mudali, Electrochemical and surface investigation of zirconium based metallic glass $Zr_{59}Ti_3Cu_{20}Al_{10}Ni_8$ alloy in nitric acid and sodium chloride media, J. Alloy. Compd. 503 (2010) 50–56, https://doi.org/10.1016/j.jallcom.2010.05.002
[121] Y.F. Zheng, X.N. Gu, F. Witte, Biodegradable metals, Mater. Sci. Eng. R Rep. 77 (2014) 1–34, https://doi.org/10.1016/j.mser.2014.01.001
[122] S.N. Li, J.B. Liu, J.H. Li, J. Wang, B.X. Liu, Composition-dependent structural and electronic properties of Mg 95– x Zn x Ca 5 metallic glasses: an ab initio molecular dynamics study, J. Phys. Chem. B 119 (2015) 3608–3618, https://doi.org/10.1021/acs.jpcb.5b00400
[123] J. Liu, Y. Fu, Y. Tang, X.D. Wang, Q.P. Cao, D.X. Zhang, J.Z. Jiang, Thickness dependent structural evolution in Mg-Zn-Ca thin film metallic glasses, J. Alloy. Compd. 742 (2018) 524–535, https://doi.org/10.1016/j.jallcom.2018.01.312
[124] Z. Xu, C. Smith, S. Chen, J. Sankar, Development and microstructural characterizations of Mg–Zn–Ca alloys for biomedical applications, Mater. Sci. Eng. B 176 (2011) 1660–1665, https://doi.org/10.1016/j.mseb.2011.06.008
[125] B.P. Zhang, Y. Wang, L. Geng, Research on Mg-Zn-Ca alloy as degradable biomaterial, in: Rosario Pignatello (Ed.), Biomaterials: Physics and Chemistry, InTech, 2011, p. 13, https://doi.org/10.5772/23929
[126] B. Zhang, Y. Hou, X. Wang, Y. Wang, L. Geng, Mechanical properties, degradation performance and cytotoxicity of Mg–Zn–Ca biomedical alloys with different compositions, Mater. Sci. Eng. C 31 (2011) 1667–1673, https://doi.org/10.1016/j.msec.2011.07.015
[127] S. Farahany, H.R. Bakhsheshi-Rad, M.H. Idris, M.R. Abdul Kadir, A.F. Lotfabadi, A. Ourdjini, In-situ thermal analysis and macroscopical characterization of Mg–xCa and Mg–0.5Ca–xZn alloy systems, Thermochim. Acta 527 (2012) 180–189, https://doi.org/10.1016/j.tca.2011.10.027
[128] Y. Ortega, M.A. Monge, R. Pareja, The precipitation process in Mg–Ca–(Zn) alloys investigated by positron annihilation spectroscopy, J. Alloy. Compd. 463 (2008) 62–66, https://doi.org/10.1016/j.jallcom.2007.09.044
[129] C.J. Boehlert, K. Knittel, The microstructure, tensile properties, and creep behavior of Mg–Zn alloys containing 0–4.4wt% Zn, Mater. Sci. Eng. A 417 (2006) 315–321, https://doi.org/10.1016/j.msea.2005.11.006
[130] M.S. Dambatta, S. Izman, B. Yahaya, J.Y. Lim, D. Kurniawan, Mg-based bulk metallic glasses for biodegradable implant materials: A review on glass forming ability, mechanical properties, and biocompatibility, J. Non Cryst. Solids 426 (2015) 110–115, https://doi.org/10.1016/j.jnoncrysol.2015.07.018
[131] S.J. Chung, A. Roy, D. Hong, J.P. Leonard, P.N. Kumta, Microstructure of Mg–Zn–Ca thin film derived by pulsed laser deposition, Mater. Sci. Eng. B 176 (2011) 1690–1694, https://doi.org/10.1016/j.mseb.2011.08.006
[132] J. Li, F.S. Gittleson, Y. Liu, J. Liu, A.M. Loye, L. McMillon-Brown, T.R. Kyriakides, J. Schroers, A.D. Taylor, Exploring a wider range of Mg-Ca-Zn metallic glass as biocompatible alloys using combinatorial sputtering, Chem. Commun. 53 (2017) 8288–8291, https://doi.org/10.1039/c7cc02733h
[133] K.S. Abisegapriyan, A. Rajeshwari, S. Kundu, B. Subramanian, Magnesium glassy alloy laminated nanofibrous polymer as biodegradable scaffolds, J. Non Cryst. Solids 502 (2018) 210–217, https://doi.org/10.1016/j.jnoncrysol.2018.09.011
[134] Hans J. Griesser (Ed.), Thin Film Coatings for Biomaterials and Biomedical Applications, first ed., Woodhead Publishing, Duxford, 2016, ⟨https://www.sciencedirect.com/book/9781782424536/thin-film-coatings-for-biomaterials-and-biomedical-applications⟩.
[135] J. Chen, Chapter 7: thin film coatings and the biological interface, in: Hans Griesser (Ed.), Thin Film Coatings for Biomaterials and Biomedical Applications, first ed., Woodhead Publishing, Cambridge, 2016, pp. 143–164, https://doi.org/10.1016/B978-1-78242-453-6.00007-9